Assessing human weaning practices with calcium isotopes in tooth enamel

Théo Tacail[a,1], Béatrice Thivichon-Prince[b,c,d], Jeremy E. Martin[a], Cyril Charles[b], Laurent Viriot[b], and Vincent Balter[a]

[a]Laboratoire de Géologie de Lyon: Terre, Planètes, et Environnement, Université de Lyon, École Normale Supérieure de Lyon, Université Lyon 1, Centre National de la Recherche Scientifique, Unité Mixte de Recherche 5276, 69364 Lyon, France; [b]Team Evolution of Vertebrate Dentition, Institut de Génomique Fonctionnelle de Lyon, École Normale Supérieure de Lyon, Centre National de la Recherche Scientifique, Unité Mixte de Recherche 5242, Université Claude Bernard Lyon 1, 69364 Lyon, France; [c]Faculté d'Odontologie, Université Claude Bernard Lyon 1, 69372 Lyon, France; and [d]Service d'Odontologie, Hospices Civils de Lyon, 69008 Lyon, France

Edited by Richard G. Klein, Stanford University, Stanford, CA, and approved April 26, 2017 (received for review March 16, 2017)

Weaning practices differ among great apes and likely diverged during the course of human evolution, but behavioral inference from the fossil record is hampered by a lack of unambiguous biomarkers. Here, we show that early-life dietary transitions are recorded in human deciduous tooth enamel as marked variations in Ca isotope ratios ($\delta^{44/42}$Ca). Using a sequential microsampling method along the enamel growth axis, we collected more than 150 enamel microsamples from 51 deciduous teeth of 12 different modern human individuals of known dietary histories, as well as nine enamel samples from permanent third molars. We measured and reconstructed the evolution of ^{44}Ca/^{42}Ca ratios in enamel from in utero development to first months of postnatal development. We show that the observed variations of $\delta^{44/42}$Ca record a transition from placental nutrition to an adult-like diet and that Ca isotopes reflect the duration of the breastfeeding period experienced by each infant. Typically, the $\delta^{44/42}$Ca values of individuals briefly or not breastfed show a systematic increase during the first 5–10 mo, whereas individuals with long breastfeeding histories display no measurable variation in $\delta^{44/42}$Ca of enamel formed during this time. The use of Ca isotope analysis in tooth enamel allows microsampling and offers an independent approach to tackle challenging questions related to past population dynamics and evolution of weaning practices in hominins.

calcium isotopes | tooth enamel | dietary transitions | weaning | breast milk

The reconstruction of weaning practices, the dietary transition from exclusive breastfeeding to exclusive nonmilk food (1), is fundamental in the study of past populations and in human evolution. Weaning constitutes a major determinant in health and survival of mammals (2–7). On the one hand, breast milk provides offspring with a safe and easily digested source of nutrients and energy together with immunological protection (5, 7–9). On the other hand, transition to nonmilk food, which supplements milk in the course of weaning, possibly exposes infants to exogenous pathogens and energy shortfalls, although its introduction is necessary to meet the growing requirements of offspring (3, 8–11). Hence, the timing of this transition constitutes the biological and behavioral pivot of a trade-off between increased juvenile survival and the recovery of maternal reproductive ability, which is delayed by lactational amenorrhea (5, 8, 9, 12, 13). Study of weaning practices can thus help characterize health, fertility, and demography of present and past human populations (5, 7, 14).

Weaning behavior is also a determinant trait in developmental biology and in evolution of life-history strategies of mammals, and humans in particular (5, 9, 12, 15, 16). Nonindustrialized modern humans are characterized by younger ages at cessation of suckling (i.e., ages at weaning) than those of great apes, namely orangutan (*Pongo* spp.), gorilla (*Gorilla* spp.), and their closest relatives, chimpanzees and bonobos (*Pan troglodytes* and *Pan paniscus*) (5, 9, 15–20). Contrary to great apes, human infants are fully weaned before independent feeding, which allows provisioning offspring with solid and processed food (5, 16). This early weaning practice is associated with other specific life-history traits, such as a later age at first female reproduction, shorter intervals between births, extended postmenopausal longevity, and a longer lifespan (5, 16, 21).

Study of past human populations including health, demography, and evolution is partly hampered by a lack of direct evidence of weaning behavior in archaeological and fossil settings. Predictions from life-history theory and indirect morphological or histological markers bring little solid insight into past weaning practices (9). Variations in chemical and isotopic composition of bone, tooth enamel, or dentine can bring information on weaning practices. Despite possible effects of dietary transition on carbon and oxygen isotope ratios of skeletal remains (see review in ref. 14), the most widely accepted biomarker for weaning practices is the nitrogen isotope ratio measured in hair, fingernails, bone, or dentine collagen (22–25). The Sr/Ca and Ba/Ca elemental ratios in tooth enamel and dentine have also proved relevant for reconstructing early-life dietary transitions (1, 26, 27). Nevertheless, these various methods are possibly associated with one or several drawbacks. The main concern is that the isotopic and elemental ratios are possibly contaminated or modified during diagenesis, depending on the burial context (28). Regarding nitrogen isotope ratios, the problem lies in the fact that the collagen fraction is not preserved beyond 100,000 y at best (29).

Ca stable isotope ratios from tooth enamel offer new perspectives on the reconstruction of weaning practices:

i) Mammal milk, especially breast milk, has extreme Ca isotope compositions with ratios significantly lighter than dietary intake, *ca.* −0.60‰ as measured for cattle, ewes, and human (30–32). The $\delta^{44/42}$Ca values in breast milk lie between −1.50 and −2.00‰ in modern humans (30), whereas the average Western diet is estimated to lie around −1.00‰ (31–33) (see Table S1 for compilation). Thus, the transition from

Significance

The practice of weaning, the dietary transition from exclusive breastfeeding to exclusive nonmilk food, is a key aspect of development and evolution of hominins, but its study in the fossil record is hampered by a lack of unambiguous biomarkers. Ca stable isotope ratios of skeletal remains are expected to bear information about milk consumption. Here we demonstrate that modern human tooth enamel records a temporal variation of Ca isotope compositions, which is related to breastfeeding duration. Ca isotopes could be used as a biomarker for reconstruction of weaning practices in past human and fossil hominin species.

Author contributions: J.E.M., C.C., L.V., and V.B. designed research; T.T. and B.T.-P. performed research; T.T. analyzed data; and T.T., B.T.-P., J.E.M., C.C., L.V., and V.B. wrote the paper.

The authors declare no conflict of interest.

This article is a PNAS Direct Submission.

[1]To whom correspondence should be addressed. Email: theo.tacail@ens-lyon.fr.

This article contains supporting information online at www.pnas.org/lookup/suppl/doi:10.1073/pnas.1704412114/-/DCSupplemental.

exclusive breast milk consumption to a child's or an adult's diet should induce a positive shift in $\delta^{44/42}$Ca values in dietary Ca of the order of +0.60‰.

ii) Ca makes up 40% in weight of hydroxylapatite, the major mineral phase of tooth dentine and enamel. This allows faintly destructive microsampling (<100 μg of enamel) and thus increases spatial resolution within incrementally structured dental tissues (34, 35).

iii) The enamel Ca isotope composition shows little sensitivity to diagenesis, even after several million years (36, 37), given that secondary Ca carbonates are leached accordingly.

The hypothesis that Ca isotopes allow tracking intake of human or animal milk was formulated earlier (30). In former studies, the focus was on the possible influence of dairy product consumption on bone Ca isotope composition. Unfortunately, results did not allow animal milk intake to be distinguished from intrinsic biological variability (38–40).

Here, we test this hypothesis by measuring $\delta^{44/42}$Ca along enamel of human deciduous teeth of modern individuals that were weaned at various known ages. Using a sequential microsampling method along the enamel growth axis, we collected more than 150 enamel microsamples from 51 deciduous teeth of 12 different modern human individuals of known dietary histories, as well as nine enamel samples from permanent third molars. The deciduous teeth set of samples stemmed from healthy individuals with various diet histories, covering three main scenarios: exclusive breastfeeding from birth, exclusive formula feeding from birth, and a breastfeeding period with subsequent formula feeding (Table 1).

Results

All 163 enamel $\delta^{44/42}$Ca values vary around a median value of −1.75‰ and range from −2.28‰ to −1.30‰, representing the very lower end of the natural accounted-for variability of Ca isotope compositions (Figs. S1 and S2 and Dataset S1).

The lowest $\delta^{44/42}$Ca values were measured in the group of prenatal enamel samples, with a median of −1.87‰ and values ranging from −2.28‰ to −1.51‰ ($n = 51$). This is in significant contrast with the higher values of the wisdom teeth group (from −1.73 ‰ to −1.34‰, average value of −1.58‰, $n = 9$) and the postnatal enamel group that covers a wider range of values (from −2.15‰ to −1.30‰, median value of −1.70‰, $n = 84$). The total range of values from enamel sampled on the neonatal line is indistinguishable from prenatal enamel, with values ranging from −2.11‰ to −1.61‰ ($n = 16$).

We observe significant differences among these groups (Fig. 1*A*; Welch's ANOVA, $P < 0.001$; Kruskal–Wallis, $P < 0.001$). More precisely, we observe a transition of Ca isotopic compositions toward ^{44}Ca-enriched values, from prenatal to postnatal development stages (Welch's t test, $P < 0.001$; Wilcoxon–Mann–Whitney, $P < 0.001$). For each measurement in a given individual, we can define a $\Delta^{44/42}$Ca value, given by the difference between the $\delta^{44/42}$Ca value of a considered spot and the average $\delta^{44/42}$Ca value of an individual's prenatal enamel. We observe for infants with no or short breastfeeding histories (less than or equal to 4 mo) an increase of the $\Delta^{44/42}$Ca value from pre- to postnatal development stages (Fig. 1*B*; Welch's ANOVA, $P < 0.001$; Kruskal–Wallis, $P < 0.001$). Conversely, we do not observe for infants with long breastfeeding histories (more than 12 mo) any significant increase of the $\Delta^{44/42}$Ca value from pre- to postnatal development stages (Fig. 1*C*; Welch's ANOVA, $P = 0.76$; Kruskal–Wallis, $P = 0.66$). At the individual level (Fig. 2 and Fig. S3), a systematic and significant increase of the $\delta^{44/42}$Ca value is observed for individuals with short or no breastfeeding history except potentially for one individual (C). No significant difference is observed for infants that were breastfed longer than 12 mo. Parametric and nonparametric statistical analyses of differences between aforementioned categories for both $\delta^{44/42}$Ca and $\Delta^{44/42}$Ca values were performed using R software (41) and are summarized in Table S2 and Fig. S3.

Discussion

Ca Isotope Composition of Adult and Prenatal Diet. The estimated average $\delta^{44/42}$Ca value of the Western diet lies around −1.00‰ (31–33), and the physiological processing of Ca results in a shift of $\delta^{44/42}$Ca from diet to bone of −0.60‰ ($\Delta_{\text{bone-diet}}$) on average (30). The $\Delta_{\text{bone-diet}}$ value is well conserved among adult mammals,

Table 1. Description of individuals' early life, dietary histories, and sampled teeth

				Breastfeeding		Formula feeding			Deciduous teeth		
ID	Sex	Year of birth	Gestation length, mo	Yes or no	Age at end, mo	Yes or no	Age at end, mo	Age at nonmilk food introduction, mo	No.	Types	Permanent teeth
A	Male	1997	9	No	—	Yes	12	4	4	m^2 - m^1 - c′ - i^1	—
G	Female	1999	8.5	No	—	Yes	12	6	5	m^2 - m^1 - c′ - i^2 - i^1	—
L	Male	1971	9	Yes	0.5	Yes	12	3	3	m^2 - m^1 - i^1	—
C	Female	1983	9.6 ± 0.4	Yes	1.7	Yes	>4	3	5	m^2 - m^1 - m_1 - c′ - i^1	M^3*
F	Male	1991	9	Yes	2	Yes	12	4	5	m^2 - m^1 - c′ - i^2 - i^1	—
K	Male	1993	9	Yes	2.5	Yes	12	4	5	m^2 - m^1 - c′ - i^2 - i^1	—
H	Female	1997	9	Yes	3.75	Yes	12	4	5	m^2 - m^1 - c′ - i^2 - i^1	—
B	Female	1992	8.75	Yes	4	No	—	3.5	4	m^2 - m^1 - c′ - i^1	—
I	Female	1979	9	Yes	4	Yes	12	5	5	m_1 - m^1 - c′ - i^2 - i^1	M^3*
D	Female	2011	NA	Yes	24	NA	NA	NA	3	m_1(L) - m_1(R) - m^1(L)	—
E	Male	2011	9	Yes	24	No	—	6	4	m_2 - m_1 - m^1 - i	—
J	Male	2009	9	Yes	36	No	—	6	3	m_1 - m^1 - c,	—
M	Female	1948	—	—	—	—	—	—	—	—	M^3*
N	Female	1981	—	—	—	—	—	—	—	—	M^3*
O	Male	1985	—	—	—	—	—	—	—	—	M^3*
P	Female	1983	—	—	—	—	—	—	—	—	M^3*
Q	Female	NA	—	—	—	—	—	—	—	—	M^3*
R	Female	1947	—	—	—	—	—	—	—	—	$M3^{\dagger}$
S	Female	1990	—	—	—	—	—	—	—	—	$M3^{\dagger}$

Individuals are sorted according to age at end of breastfeeding. NA, not available.

*Described in ref. 59.

†Described in ref. 34.

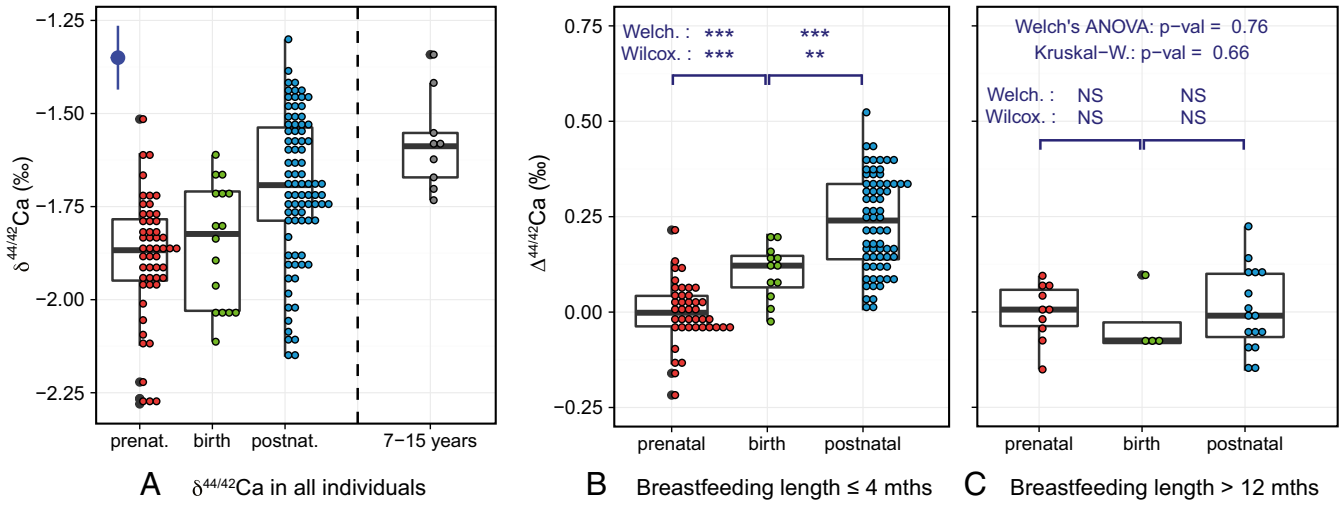

Fig. 1. (*A*) Box plot of $\delta^{44/42}$Ca values (per mil, ICP Ca Lyon) in enamel sorted by development stage categories for all individuals, corresponding to prenatal development period, birth, postnatal development period, and wisdom teeth enamel formation (i.e., 7–15 y of age). Error bar represents average 2 SD. (*B* and *C*) Box plots represent $\Delta^{44/42}$Ca values ($\delta^{44/42}Ca_{sample} - \delta^{44/42}Ca_{prenatal\ average}$, for a given individual) calculated for individuals with short breastfeeding histories (*B*, less than or equal to 4 mo, $n = 9$) and longer breastfeeding histories (*C*, longer than 12 mo, $n = 3$). *P* values of Welch's unequal variance *t* tests, Wilcoxon–Mann–Whitney test, Welch's ANOVA, and Kruskal–Wallis tests are given here and summarized in Table S2. NS, nonsignificant *P* value; $*P = 0.01–0.05$; $**P = 0.001–0.01$; and $***P < 0.001$.

including horses, seals, mice, deer, sheep, and Göttingen minipigs (30, 42–45) and is assumed to be comparable in humans (46, 47). The average $\delta^{44/42}$Ca value of wisdom tooth enamel that we measured in nine adult individuals (−1.58 ± 0.26 ‰, 2 SD, $n = 9$) is thus in good agreement with a hypothetical average Western diet composition of −1.00‰. An individual 7–15 y of age has a diet near or identical to that of an adult and this is thus compatible with our observations in wisdom tooth enamel, known to grow during this period.

Enamel that initiates formation early, that is, during the second and third trimesters of in utero development (48), is characterized by a ^{44}Ca-depleted isotope composition compared with third molar enamel (Welch *t* test, $P < 0.001$; Wilcoxon–Mann–Whitney, $P < 0.001$) and has a mean $\delta^{44/42}$Ca lower than that of third molars by −0.31 ± 0.11 ‰ (Welch *t* test 95% confidence interval). Such a ^{44}Ca-depleted isotope composition in fetus enamel has several possible and likely combined causes. First, compared with the estimated −1.00‰ mean value of diet, the mother's blood has lower $\delta^{44/42}$Ca values: a compilation of available data in mammals yields a Ca isotopic shift value from diet to blood, denoted $\Delta_{blood\text{-}diet}$ and given by the difference between $\delta^{44/42}Ca_{blood}$ and $\delta^{44/42}Ca_{diet}$, of −0.30 ± 0.13 ‰ (1 SD, Table S3). Second, increased bone turnover and possible transient bone loss in pregnant women (49, 50) could also involve a decrease in blood $\delta^{44/42}$Ca values (46, 47). Third, the transfer of Ca from maternal to fetal blood involves an active transport of Ca through the placenta (51), hypothetically responsible for preferential transport of light Ca isotopes (32, 33). Fourth, metabolism of the fetus itself, notably involving mineralization, could explain a further decrease in $\delta^{44/42}$Ca from source Ca to mineralized tissues (42).

Despite these possible explanations for a ^{44}Ca-depleted isotope composition of fetus enamel, the calculated $\Delta_{blood\text{-}diet}$ value (*ca.* −0.3‰) perfectly matches the observed difference between the $\delta^{44/42}$Ca values of wisdom tooth enamel (−1.58‰), representative of the adult diet, and the $\delta^{44/42}$Ca values of prenatal enamel (−1.87‰), representative of the mother's blood. This result supports the interpretation that the observed long-term $\delta^{44/42}$Ca shift from in utero enamel to wisdom tooth enamel mainly reflects a dietary transition in Ca uptake from mother's blood to adult diet.

Ca Isotope Composition of Postnatal Diet and Influence of Breastfeeding. The drift in Ca isotope compositions is related to the duration of breast milk intake. Introduction of human milk at birth involves a source of Ca with a highly ^{44}Ca-depleted isotope composition (∼−1.6‰; see Table S1). The explanations for such low $\delta^{44/42}$Ca values in breast milk are multiple. First, as discussed above, mother's blood has a Ca isotope composition lower than that of the diet by the order of −0.30‰. Second, the transfer of Ca to milk involves active transportation through mammary epithelium (52), which is thought to account for a preferential secretion of light Ca isotopes (30, 32). Third, lactation is known to involve an increased mobilization of light skeletal Ca in the mother (49) that could induce a decrease in mother's blood $\delta^{44/42}$Ca (46, 47). The transition from prenatal diet (i.e., mother's blood) to breastfeeding should thus not be accompanied by a significant isotopic shift toward ^{44}Ca-enriched compositions, the human $\delta^{44/42}Ca_{blood}$ value being quite ^{44}Ca-depleted, somewhere around −1.3‰ (Table S1). This assumption is matched in the three infants breastfed for a longer period. Individuals that were breastfed more than 12 mo (24, 24, and 36 mo for individuals D, E, and J, respectively; Figs. 1*C* and 2 and Fig. S3) do not display significant positive deviations in Ca isotope compositions, either at birth or in postnatal enamel (Welch's ANOVA, $P = 0.76$; Kruskal–Wallis, $P = 0.66$). Postnatal enamel in these individuals is indistinguishable from prenatal enamel (Welch's *t* test, $P = 0.89$, shift of + 0.00 ± 0.07‰, 95% confidence interval; Wilcoxon–Mann–Whitney, $P = 0.98$), whereas the long-term amplitude of isotopic deviation between postnatal enamel of these individuals and third molar enamel yields a value of + 0.33 ± 0.11‰ (Welch's *t* test, $P < 0.001$, 95% confidence interval). The postnatal duration that was sampled in tooth enamel for each of these individuals is lower than 10 mo and thus was markedly shorter than their ages at cessation of suckling, known to be 24 and 36 mo. This confirms the hypothesis first formulated 10 y ago (30) that breast milk consumption is recorded within human deciduous tooth enamel.

With the exception of individual C, postnatal enamel of all other briefly breastfed or not breastfed individuals displays significantly higher $\delta^{44/42}$Ca values than enamel contemporary to birth and prenatal enamel. For each of these individuals, the sampled postnatal estimated time period equals or exceeds the first 5 mo after birth. This is in agreement with a dietary change of Ca intake from placental nutrition to an infant breast milk-free diet within a timeframe of 0–4 mo (Table 1).

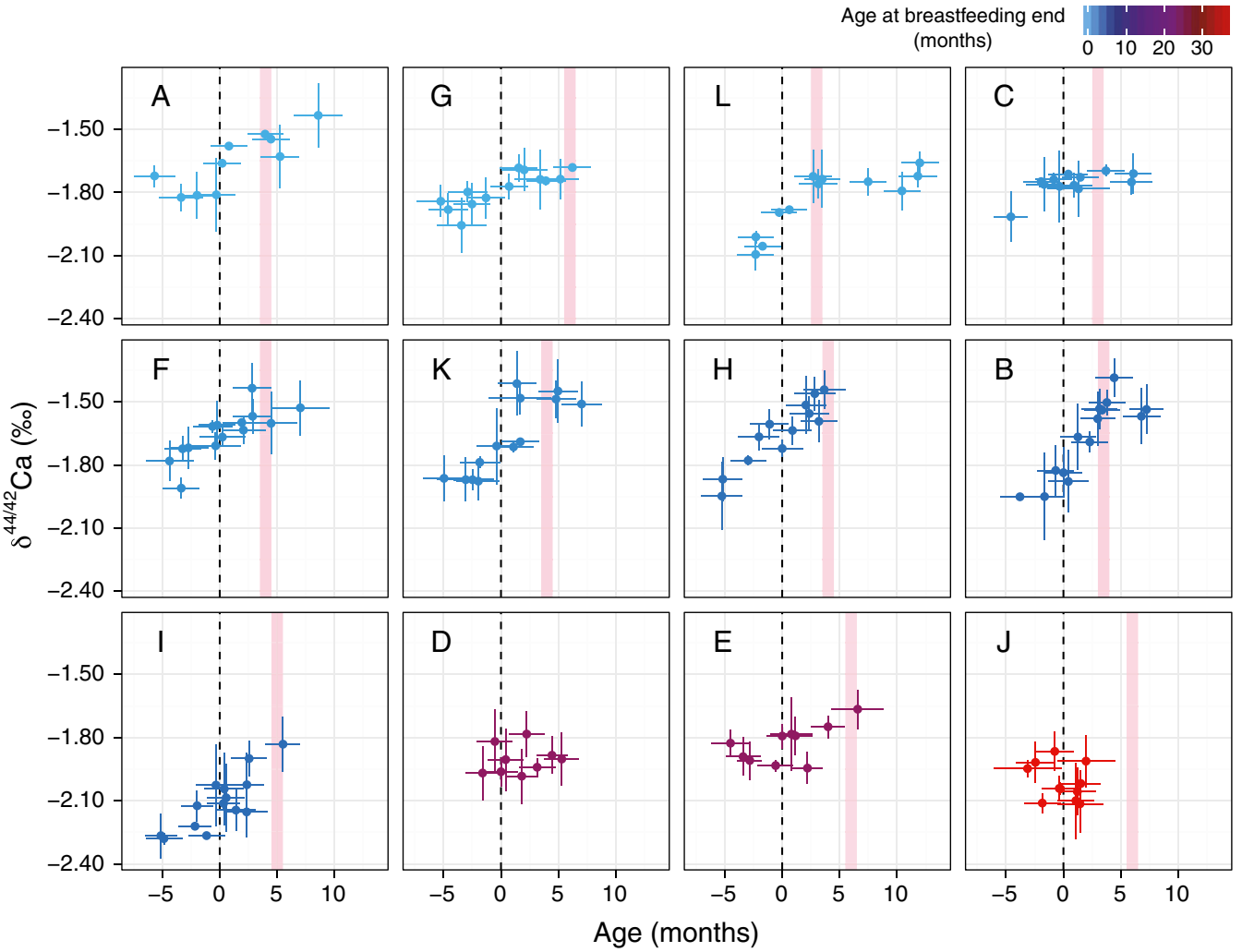

Fig. 2. (*A–L*) Temporal evolution of $\delta^{44/42}$Ca values (per mil, ICP Ca Lyon) in each individual. Individuals are sorted by increasing age at breastfeeding cessation (months). Color scale corresponds to age at cessation of breastfeeding. Vertical error bars are 2 SD and horizontal error bars are estimated time envelopes. Black dashed vertical lines mark birth; red shaded areas cover periods of introduction of nonmilk food (age at diversification ± 0.5 mo).

Residual Variability of Ca Isotope Compositions. In briefly breastfed individuals (all except D, E, and J) no clear and precise relationship appears between the duration of the breastfeeding period (from 0 to 4 mo) and the value of $\Delta^{44/42}$Ca in postnatal enamel. In other words, the value of the slope is not correlated with the duration of the breastfeeding period. Several explanations can be put forward.

First, all non-breastfed or briefly breastfed individuals were subsequently fed with various infant formulas, except for individual B. Substitute milk or infant formulas have high Ca levels resulting from various mixtures of animal milk and whey, inorganic Ca, and, possibly, vegetables. Their average isotope compositions are variable (15 different infant formulas analyzed for $\delta^{44/42}$Ca range between −0.82 and −0.01‰) and ^{44}Ca-enriched compared with breast milk considering the origin of Ca in these ingredients (average $\delta^{44/42}$Ca of −0.49 ± 0.51‰, 2 SD, Table S1). The same holds true for transition alimentation that is composed of various dairy and vegetable components with average ^{44}Ca-enriched compositions. The amplitude of the shift between the prenatal period and the period of milk-free food intake is thus likely variable depending on transition food types and on formula compositions. The study of more simple dietary histories, such as in captive macaques (1), would facilitate discerning patterns with finer time and amplitude resolutions.

Second, the spatial resolution that the sampling method allows is about 400 μm, which corresponds to 2.4- to 4.4-mo time envelopes, depending on enamel secretion rates. This temporal resolution likely induces a dampening of steep variations, such as experienced by individual B.

Third, the maturation of newly formed enamel (53, 54) possibly generates elemental and isotopic mixing between initially secreted enamel and secondary matured enamel, which could participate in a dampening and a phase shifting of the recorded signal (55). The improvement of the estimation of the timing of dietary transition would thus benefit from a comprehensive investigation of the transduction of Ca isotope signal from dietary intake to enamel such as in hypsodont herbivores.

Implications for Trophic-Level Reconstruction Using $\delta^{44/42}$Ca of Mammalian Tooth Enamel. Trophic-level studies in modern and past environments using Ca isotopes are promising but are confronted with poorly understood residual variability both in terrestrial and marine environments (37, 56). These studies are based on observed isotopic offsets in $\delta^{44/42}$Ca varying between −0.14‰ and −0.65‰ from one trophic level to another (37, 42, 57). This is of a magnitude comparable to the shift observed here from prenatal or exclusive breast milk to a breast milk-free diet (∼ +0.30‰). The consumption of breast milk is likely to induce

a difference in the Ca isotope composition of enamel that could be confused with a signature of a superior trophic level.

Perspectives. The present approach allows distinguishing weaning practices in modern humans as recorded in deciduous tooth enamel. In this case, it allows distinguishing a cessation of suckling occurring within the first year, representative of weaning practices in Europe (6), from a behavior resembling early-weaning of nonindustrialized modern human, occurring between 2 and 3 y old (5, 9, 16).

We emphasize that potential applications to past human populations and extinct hominins could help in studying their weaning practices. Provided a good knowledge of enamel crown development in studied individuals, Ca isotope compositions could help determine age at significant reduction of suckling with a temporal resolution of the order of 6–12 mo. Present-day humans wean their infants earlier (2–3 y) than do great apes (3–7 y) (5, 9, 16). Whether the common ancestor of hominins was characterized by an older age at cessation of suckling than modern humans remains a matter of debate (5, 16, 19, 20) based on rather indirect inferences (9). Ca isotope studies offer an independent approach to test such hypotheses.

Materials

A total of 51 deciduous teeth from 12 healthy European children born between 1971 and 2011 were used in this study (Table 1). For each individual, three to five deciduous teeth were selected depending on available teeth, to cover the widest time span of enamel crown formation. This period corresponds to the timing of tooth crown formation in human deciduous teeth, which initiates on average at about 5 mo before birth (48) and concludes at around 1.5 y of postnatal age (58). All teeth were naturally shed or extracted for surgical purposes in accordance with the World Medical Association's Declaration of Helsinki. In each case, the informed consent of the patients or their parents was collected. Information concerning early diet was provided retrospectively by the parents when possible. We also used nine permanent third molars, initially described elsewhere (34, 59), for which crown enamel forms between 7 and 15 y of age (58), to assess the long-term trend of Ca isotope composition evolution of enamel. All teeth were collected without identifying data. Details about all individuals' early-life diet and sampled teeth are given in Table 1.

Methods

Sampling. Each permanent and deciduous tooth was halved longitudinally along the buccolingual plane using a low-speed rotating diamond saw. One half of each tooth was then embedded in araldite resin and the cut surface was polished using sandpaper with decreasing grain sizes. The sampling was performed using a precise position drilling MicroMill device allowing sampling of 60–80 μg hydroxylapatite and drilling holes of 350–400 μm in diameter and 200–300 μm in depth, as described in Tacail et al. (34) and in *Supporting Information*.

The sampling strategy consisted of drilling a series of spots with the widest possible time span available on enamel surface of the buccal side in general. Sampling was thus performed in deciduous teeth at regular intervals along the crown height (i.e., from enamel cusp to cervix). Teeth displaying substantial enamel thickness such as deciduous first and second molars allowed in some cases sampling of more than one sample from the enamel–dentine junction to the outer surface. A single enamel sample per wisdom tooth was obtained likewise (*Supporting Information*).

Location of Spots and Estimation of Mean Formation Ages of Sampled Enamel. The neonatal line is used to distinguish between enamel formed prenatally from enamel formed postnatally (60–63) (see drawings on pictures using Adobe Photoshop software, Fig. S4 and *Supporting Information*). On this basis, we split samples into three categories according to their position relative to the neonatal line: (*i*) more than 60% of the sampling spot surface lies in prenatal enamel, (*ii*) more than 60% of the sampling spot surface lies in postnatal enamel, and (*iii*) less than 60% of the sampling spot surface lies in either of the pre- or postnatal enamel, referred to here as birth category. We also measured the distance of each sampling spot to neonatal line along the main prism orientation and thus propose a first-order age model for sampled enamel assuming an average enamel secretion rate of 4 $\mu m \cdot d^{-1}$ for all teeth together (48, 64, 65) (*Supporting Information*).

Sample Preparation and $\delta^{44/42}$Ca Measurement. After collection, each powder sample was chemically purified following method described elsewhere (44) and in *Supporting Information*. The measurement of Ca isotope compositions was performed at the Laboratoire de Géologie de Lyon, France, on a Neptune Plus multicollector induced coupled plasma mass spectrometer (MC-ICP-MS) from Thermo Scientific using a previously described protocol (34, 44) (Fig. S1, Table S4, and *Supporting Information*). All Ca isotope compositions are expressed in per mil units, using the "delta" notation for the $^{44}Ca/^{42}Ca$ isotope ratios defined as follows:

$$\delta^{44/42}\mathrm{Ca} = \left(\frac{\left(^{44}\mathrm{Ca}/^{42}\mathrm{Ca}\right)_{\mathrm{sample}}}{\left(^{44}\mathrm{Ca}/^{42}\mathrm{Ca}\right)_{\mathrm{ICP\ Ca\ Lyon}}} - 1 \right) \times 1{,}000,$$

where $(^{44}Ca/^{42}Ca)_{sample}$ and $(^{44}Ca/^{42}Ca)_{ICP\ Ca\ Lyon}$ are Ca isotope abundance ratios measured in sample and in ICP Ca Lyon bracketing standard, respectively.

ACKNOWLEDGMENTS. We thank E. Albalat and P. Télouk for analytical advice, Dr. P. Dorr for providing tooth samples, and D. Mollex for help in sample preparation. This work was supported by the Fondation Bullukian, the Fondation Mérieux, and the Fonds Recherche of the Ecole Normale Supérieure de Lyon ("No Milk Today" project). The authors are grateful to the LABEX Lyon Institute of Origins (ANR-10-LABX-0066) of the Université de Lyon for its financial support within the program "Investissements d'Avenir" (ANR-11-IDEX-0007) of the French government operated by the National Research Agency (ANR).

1. Austin C, et al. (2013) Barium distributions in teeth reveal early-life dietary transitions in primates. *Nature* 498:216–219.
2. Dettwyler KA, Fishman C (1992) Infant feeding practices and growth. *Annu Rev Anthropol* 21:171–204.
3. Michaelsen KF, Friis H (1998) Complementary feeding: A global perspective. *Nutrition* 14:763–766.
4. Ip S, et al. (2007) Breastfeeding and maternal and infant health outcomes in developed countries. *Evid Rep Technol Assess (Full Rep)* 18:1–186.
5. Sellen DW (2007) Evolution of infant and young child feeding: Implications for contemporary public health. *Annu Rev Nutr* 27:123–148.
6. WHO (2009) Infant and young child feeding: Model Chapter for textbooks for medical students and allied health professionals. Available at apps.who.int/iris/bitstream/10665/44117/1/9789241597494_eng.pdf.
7. Lönnerdal B (2000) Breast milk: A truly functional food. *Nutrition* 16:509–511.
8. McDade TW (2003) Life history theory and the immune system: Steps toward a human ecological immunology. *Am J Phys Anthropol* 122:100–125.
9. Humphrey LT (2010) Weaning behaviour in human evolution. *Semin Cell Dev Biol* 21:453–461.
10. WHO (1998) Complementary feeding of young children in developing countries: A review of current scientific knowledge. Available at www.who.int/nutrition/publications/infantfeeding/WHO_NUT_98.1/en/. Accessed January 25, 2017.
11. Dewey KG, Brown KH (2003) Update on technical issues concerning complementary feeding of young children in developing countries and implications for intervention programs. *Food Nutr Bull* 24:5–28.
12. Lee PC (1996) The meanings of weaning: Growth, lactation, and life history. *Evol Anthropol* 5:87–98.
13. Valeggia C, Ellison PT (2009) Interactions between metabolic and reproductive functions in the resumption of postpartum fecundity. *Am J Hum Biol* 21:559–566.
14. Tsutaya T, Yoneda M (2015) Reconstruction of breastfeeding and weaning practices using stable isotope and trace element analyses: A review. *Am J Phys Anthropol* 156:2–21.
15. Lee PC (2012) Growth and investment in hominin life history evolution: Patterns, processes, and outcomes. *Int J Primatol* 33:1309–1331.
16. Van Noordwijk MA, Kuzawa CW, Van Schaik CP (2013) The evolution of the patterning of human lactation: A comparative perspective. *Evol Anthropol* 22:202–212.
17. Galdikas BMF, Wood JW (1990) Birth spacing patterns in humans and apes. *Am J Phys Anthropol* 83:185–191.
18. Bogin B, Smith BH (1996) Evolution of the human life cycle. *Am J Hum Biol* 8:703–716.
19. Kennedy GE (2005) From the ape's dilemma to the weanling's dilemma: Early weaning and its evolutionary context. *J Hum Evol* 48:123–145.
20. Robson SL, Wood B (2008) Hominin life history: Reconstruction and evolution. *J Anat* 212:394–425.
21. Kachel AF, Premo LS, Hublin J-J (2011) Modeling the effects of weaning age on length of female reproductive period: Implications for the evolution of human life history. *Am J Hum Biol* 23:479–487.
22. Fogel ML (1989) Nitrogen isotope tracers of human lactatino in modern and archeological populations. *Carnegie Institute of Washington Yearbook* (Carnegie Institute of Washington, Washington, DC), Vol 88, pp 111–117.
23. Fuller BT, Fuller JL, Harris DA, Hedges REM (2006) Detection of breastfeeding and weaning in modern human infants with carbon and nitrogen stable isotope ratios. *Am J Phys Anthropol* 129:279–293.
24. Jenkins SG, Partridge ST, Stephenson TR, Farley SD, Robbins CT (2001) Nitrogen and carbon isotope fractionation between mothers, neonates, and nursing offspring. *Oecologia* 129:336–341.

25. Reynard LM, Tuross N (2015) The known, the unknown and the unknowable: Weaning times from archaeological bones using nitrogen isotope ratios. *J Archaeol Sci* 53:618–625.
26. Humphrey LT, Dirks W, Dean MC, Jeffries TE (2008) Tracking dietary transitions in weanling baboons (*Papio hamadryas anubis*) using strontium/calcium ratios in enamel. *Folia Primatol (Basel)* 79:197–212.
27. Humphrey LT, Dean MC, Jeffries TE, Penn M (2008) Unlocking evidence of early diet from tooth enamel. *Proc Natl Acad Sci USA* 105:6834–6839.
28. Reynard B, Balter V (2014) Trace elements and their isotopes in bones and teeth: Diet, environments, diagenesis, and dating of archeological and paleontological samples. *Palaeogeogr Palaeoclimatol Palaeoecol* 416:4–16.
29. Koch PL (2007) Isotopic study of the biology of modern and fossil vertebrates. *Stable Isotopes in Ecology and Environmental Science*, eds Michener R, Lajtha K (Blackwell, Boston), 2nd Ed, pp 99–154.
30. Chu N-C, Henderson GM, Belshaw NS, Hedges REM (2006) Establishing the potential of Ca isotopes as proxy for consumption of dairy products. *Appl Geochem* 21: 1656–1667.
31. Gussone N, Heuser A (2016) Biominerals and biomaterial. *Calcium Stable Isotope Geochemistry* (Springer, Berlin), pp 111–144.
32. Heuser A (2016) Biomedical application of Ca stable isotopes. *Calcium Stable Isotope Geochemistry* (Springer, Berlin), pp 247–260.
33. Heuser A, Eisenhauer A (2010) A pilot study on the use of natural calcium isotope (44Ca/40Ca) fractionation in urine as a proxy for the human body calcium balance. *Bone* 46:889–896.
34. Tacail T, Télouk P, Balter V (2016) Precise analysis of calcium stable isotope variations in biological apatites using laser ablation MC-ICPMS. *J Anal At Spectrom* 31:152–162.
35. Li Q, Thirlwall M, Müller W (2016) Ca isotopic analysis of laser-cut microsamples of (bio)apatite without chemical purification. *Chem Geol* 422:1–12.
36. Heuser A, Tütken T, Gussone N, Galer SJG (2011) Calcium isotopes in fossil bones and teeth—Diagenetic versus biogenic origin. *Geochim Cosmochim Acta* 75:3419–3433.
37. Martin JE, Tacail T, Adnet S, Girard C, Balter V (2015) Calcium isotopes reveal the trophic position of extant and fossil elasmobranchs. *Chem Geol* 415:118–125.
38. Reynard LM, Henderson GM, Hedges REM (2010) Calcium isotope ratios in animal and human bone. *Geochim Cosmochim Acta* 74:3735–3750.
39. Reynard LM, Henderson GM, Hedges REM (2011) Calcium isotopes in archaeological bones and their relationship to dairy consumption. *J Archaeol Sci* 38:657–664.
40. Reynard LM, Pearson JA, Henderson GM, Hedges REM (2013) Calcium isotopes in juvenile milk-consumers. *Archaeometry* 55:946–957.
41. R Core Team (2016) R: A language and environment for statistical computing (R Foundation for Statistical Computing, Vienna). Available at www.r-project.org/.
42. Skulan J, DePaolo DJ (1999) Calcium isotope fractionation between soft and mineralized tissues as a monitor of calcium use in vertebrates. *Proc Natl Acad Sci USA* 96: 13709–13713.
43. Hirata T, et al. (2008) Isotopic analysis of calcium in blood plasma and bone from mouse samples by multiple collector-ICP-mass spectrometry. *Anal Sci* 24:1501–1507.
44. Tacail T, Albalat E, Télouk P, Balter V (2014) A simplified protocol for measurement of Ca isotopes in biological samples. *J Anal At Spectrom* 29:529–535.
45. Heuser A, Eisenhauer A, Scholz-Ahrens KE, Schrezenmeir J (2016) Biological fractionation of stable Ca isotopes in Göttingen minipigs as a physiological model for Ca homeostasis in humans. *Isotopes Environ Health Stud* 52:633–648.
46. Morgan JLL, et al. (2012) Rapidly assessing changes in bone mineral balance using natural stable calcium isotopes. *Proc Natl Acad Sci USA* 109:9989–9994.
47. Channon MB, et al. (2015) Using natural, stable calcium isotopes of human blood to detect and monitor changes in bone mineral balance. *Bone* 77:69–74.
48. Mahoney P (2015) Dental fast track: Prenatal enamel growth, incisor eruption, and weaning in human infants. *Am J Phys Anthropol* 156:407–421.
49. Kovacs CS, Fuleihan Gel-H (2006) Calcium and bone disorders during pregnancy and lactation. *Endocrinol Metab Clin North Am* 35:21–51, v.
50. Salles JP (2016) Bone metabolism during pregnancy. *Ann Endocrinol (Paris)* 77: 163–168.
51. Kovacs CS, Kronenberg HM (1997) Maternal-fetal calcium and bone metabolism during pregnancy, puerperium, and lactation. *Endocr Rev* 18:832–872.
52. Cross BM, Breitwieser GE, Reinhardt TA, Rao R (2014) Cellular calcium dynamics in lactation and breast cancer: from physiology to pathology. *Am J Physiol Cell Physiol* 306:C515–C526.
53. Hubbard MJ (2000) Calcium transport across the dental enamel epithelium. *Crit Rev Oral Biol Med* 11:437–466.
54. Robinson C (2014) Enamel maturation: A brief background with implications for some enamel dysplasias. *Front Physiol* 5:388.
55. Passey BH, et al. (2005) Inverse methods for estimating primary input signals from time-averaged isotope profiles. *Geochim Cosmochim Acta* 69:4101–4116.
56. Melin AD, et al. (2014) Technical note: Calcium and carbon stable isotope ratios as paleodietary indicators. *Am J Phys Anthropol* 154:633–643.
57. DePaolo D (2004) Calcium isotopic variations produced by biological, kinetic, radiogenic and nucleosynthetic processes. *Rev Mineral Geochem* 55:255–288.
58. AlQahtani SJ, Hector MP, Liversidge HM (2010) Brief communication: The London atlas of human tooth development and eruption. *Am J Phys Anthropol* 142:481–490.
59. Jaouen K, Herrscher E, Balter V (2017) Copper and zinc isotope ratios in human bone and enamel. *Am J Phys Anthropol* 162:491–500.
60. Dean MC, Beynon AD (1991) Histological reconstruction of crown formation times and initial root formation times in a modern human child. *Am J Phys Anthropol* 86: 215–228.
61. FitzGerald CM, Saunders SR (2005) Test of histological methods of determining chronology of accentuated striae in deciduous teeth. *Am J Phys Anthropol* 127: 277–290.
62. FitzGerald C, Saunders S, Bondioli L, Macchiarelli R (2006) Health of infants in an Imperial Roman skeletal sample: Perspective from dental microstructure. *Am J Phys Anthropol* 130:179–189.
63. Birch W, Dean MC (2014) A method of calculating human deciduous crown formation times and of estimating the chronological ages of stressful events occurring during deciduous enamel formation. *J Forensic Leg Med* 22:127–144.
64. Mahoney P (2011) Human deciduous mandibular molar incremental enamel development. *Am J Phys Anthropol* 144:204–214.
65. Mahoney P (2012) Incremental enamel development in modern human deciduous anterior teeth. *Am J Phys Anthropol* 147:637–651.
66. Żądzińska E, Lorkiewicz W, Kurek M, Borowska-Strugińska B (2015) Accentuated lines in the enamel of primary incisors from skeletal remains: A contribution to the explanation of early childhood mortality in a medieval population from Poland. *Am J Phys Anthropol* 157:402–410.
67. Albarède F, Telouk P, Lamboux A, Jaouen K, Balter V (2011) Isotopic evidence of unaccounted for Fe and Cu erythropoietic pathways. *Metallomics* 3:926–933.
68. Heuser A, Eisenhauer A (2008) The calcium isotope composition (δ 44/40 Ca) of NIST SRM 915b and NIST SRM 1486. *Geostand Geoanal Res* 32:311–315.
69. Morgan JLL, et al. (2011) High-precision measurement of variations in calcium isotope ratios in urine by multiple collector inductively coupled plasma mass spectrometry. *Anal Chem* 83:6956–6962.
70. Schmitt A-D (2016) Earth-surface Ca isotopic fractionations. *Calcium Stable Isotope Geochemistry* (Springer, Berlin), pp 145–172.

Supporting Information

Tacail et al. 10.1073/pnas.1704412114

Sampling

The sampling of enamel was performed using the method described in Tacail et al. (34). Briefly, it consisted of drilling the enamel surface using a tungsten carbide drill mounted on a precise position drilling MicroMill device. Drill holes were typically 350–400 μm in diameter and 200–300 μm in depth. Small powder heaps accumulated on the rims of the holes were collected using razorblades and transferred to trace-level clean Savillex vials. Before each sampling, enamel surface, drill bits and razorblades were washed and wiped using 99% pure ethanol and blown off using a compressed air duster. Each typical drill spot allowed recovery of ∼60–80 μg hydroxylapatite corresponding to about 22–30 μg of Ca. Depending on available enamel thickness relative to drill size, we performed sampling by drilling one spot or two smaller and shallower contiguous spots.

We checked for the absence of any sampling method bias on Ca isotope composition measurement. We performed microsampling under the same conditions as for teeth using SRM1400 SPS, a sintered powder bone standard (34). The two recovered powder samples were chemically purified and analyzed as unknown samples during Ca isotope composition measurement sessions.

With the exception of individuals R and S, all wisdom teeth were sampled using the same drilling method as for deciduous teeth. We performed two drilling holes in thickness of enamel cusp (near the dentin–enamel junction and close to the outer surface) and pooled the two sampled powder heaps for each individual to assess an average composition of tooth enamel. Individuals R and S (previously described in ref. 34 as BMM3 and HPME) were sampled by recovering chips of broken enamel crown.

Location of Spots and Measurement of Distance to Neonatal Line

After sampling, teeth were further smoothly polished using alumina suspensions of decreasing particle sizes, up to 0.1 μm. Direct observations were performed together with pictures taken with the help of a computer-assisted binocular microscope. The neonatal line, which is a marked stria that forms at birth in all deciduous teeth and can occur in some permanent first molars, separates pre- from postnatal enamel (60–63). The neonatal line is used to distinguish enamel formed prenatally from enamel formed postnatally (see drawings on pictures using Adobe Photoshop software, Fig. S4). On this basis, we split samples into three categories according to their position relative to the neonatal line: (*i*) more than 60% of the sampling spot surface lies in prenatal enamel, (*ii*) more than 60% of the sampling spot surface lies in postnatal enamel, and (*iii*) less than 60% of the sampling spot surface lies in either of the pre- or postnatal enamel, referred here to as birth category.

We also identified and mapped the main direction of enamel prisms and located observable accentuated incremental markings, often corresponding to postnatal stress events (61, 63, 66). We measured the distance along the main prism orientation from neonatal line to sampling spot center. Distances of sampling spot centers to neonatal lines were either measured directly or with the help of accentuated markings to estimate cumulated distances to neonatal line for sampling spots with remote locations. Accentuated growth lines were not always observed, which necessitated inferring isochronous lines according to the general geometry of the sectioned tooth. In the cases of six strictly postnatal sampling spots, distinguished in Dataset S1, their location was too imprecise or remote from the neonatal line to allow a confident estimation of distance. These samples were rejected for temporal evolution of $\delta^{44/42}$Ca presented in Fig. 2 but kept in the postnatal enamel category. Annotated pictures of all sampled teeth are presented in Fig. S4.

We then calculated a first-order estimate of chronological age assuming an average enamel secretion rate of 4 $\mu m \cdot d^{-1}$ for all teeth together (48, 64, 65). Each spot was thus associated with an estimate of the age at enamel formation with respect to birth. Also, we measured maximum sampling spot width along the prism direction and calculated for each spot the time envelope that each sampling spot encompasses.

We thus propose a first-order age model for each individual, sufficient to discuss main features of Ca isotope variation provided the sampling spatial resolution is of 400 μm on average, reflecting 2.4- to 4.4-mo periods depending on enamel secretion rates of a given tooth or crown sector (48, 64, 65).

Chemical Processing of Samples

Briefly, every sample was dissolved in subboiled distilled 1 N HCl acid and processed through AG50X-W12 cation exchange resin in 1 N HCl medium to dispose of sample matrix (i.e., phosphates, sulfates, alkali elements, and Mg). Ca and Sr fractions were collected in 6 N HCl medium. Ca fractions were then separated from Sr by loading samples onto columns filled with Sr-specific resin (Eichrom Sr-Spec) in subboiled distilled 2 N HNO_3 medium (34, 44). Blanks for the whole procedure did not exceed 100 ng Ca (44). This is 200 times smaller than smallest processed Ca samples (about 20 μg) and could not affect the measured isotopic compositions beyond the measurement precision.

A series of 15 different infant formulas from various trademarks (Table S1) were also sampled. One breast milk sample was obtained from a 36-y-old lactating French woman. Whole milk powder standard is BCR 380-R provided by Institute for Reference Materials and Measurements. The whole blood samples were collected from two French individuals residing in Lyon, France (described in ref. 67). The chemical preparation of milk and whole blood samples was performed as described elsewhere (44). Briefly, after mineralization using concentrated subboiled distilled HNO_3 acid and H_2O_2 30% Suprapur, samples were processed through AG50W-X12 cationic resin for recovery of Ca, Sr, and Fe. Ca was then separated from Fe by processing samples through AG1-X8 anionic resin before removing Sr using Sr-specific resin.

MC-ICP-MS Analysis

A standard-sample bracketing measurement method was used with the ICP Ca Lyon standard (44) as bracketing standard. Measurements of all samples and standards were performed during six sessions, between 2015 and 2017. When $\delta^{43/42}$Ca values of all measured materials are plotted as a function of their $\delta^{44/42}$Ca values, compositions fall on a line in good agreement with the 0.507 slope predicted by the linear approximation of exponential mass-dependent fractionation (Fig. S1).

The measurements were systematically checked for long-term precision and accuracy using SRM1486 bone meal NIST secondary standard previously described and analyzed for Ca isotope compositions (34, 36, 37, 44, 68). SRM1486 yielded constant values across the six different analysis sessions, with an average $\delta^{44/42}$Ca value of -1.03 ± 0.01 ‰ (2 SE, $n = 147$), in very good agreement with previously published values (as listed in Table S4), notably -1.03 ± 0.01 ‰ (2 SE, $n = 120$) (34). We also analyzed the commonly used SRM915a and SRM915b clinical-grade carbonate standards, as well as BCR-380R cow whole milk powder standard and ICP1 Ca solution used as standard in former studies (46, 47, 69). All measured $\delta^{44/42}$Ca values of standards and previously

published compositions are given for comparison in Table S4. Long-term external precision was estimated using the SRM1486 standard and yields a 2 SD value of 0.12‰ for $\delta^{44/42}$Ca for 147 analyses, over the six different sessions.

As was previously shown (34), the microsampling method did not affect measured isotope compositions of Ca. The two SRM1400 SPS microdrilled samples did not show significant differences compared with the previously published $\delta^{44/42}$Ca value of -1.24 ± 0.13 ‰ (2 SD, $n = 26$) (34): SRM1400 SPS 1 and 2 yielded indistinguishable values of -1.23 ± 0.08 ‰ (2SD, $n = 3$) and -1.27 ± 0.06 ‰ (2 SD, $n = 5$), respectively (Table S4).

Conversions of literature values expressed relative to SRM915a reference standard were performed as follows. All $\delta^{44/40}$Ca data were converted to $\delta^{44/42}$Ca values by dividing by a 1.9996 factor, calculated using the power fractionation law. The $\delta^{44/42}$Ca values were then converted to $\delta^{44/42}$Ca relative to ICP Ca Lyon using a value of SRM915a relative to ICP Ca Lyon of −0.52‰ as measured in the present study and estimated in Martin et al. (37) (Table S4). Data stemming from Channon et al. (47) were converted to ICP Ca Lyon using the measured −0.20‰ value of ICP1 Ca solution used as reference material by these authors (Tables S1 and S4). This −0.20‰ value of ICP1 Ca solution is in good agreement with the +0.05‰ published SRM915b value against ICP1, which corresponds, once converted to ICP Ca Lyon, to −0.15‰, indistinguishable from our measured composition of SRM915b.

Table S1. Ca isotope composition of cow dairy products, human breast milk (30, 31), 15 different infant formulas (this study), human whole blood (47), and estimation of average Ca isotope composition of typical Western diet and vegan Western diet (31–33)

Material	$\delta^{44/42}$Ca (relative to ICP Ca Lyon), ‰ ± 2 SD		*n*	Source
Cow milk and dairy products				
Milk	−1.19	0.14	3	Ref. 30
Whey	−1.12	0.12	2	Ref. 30
Curd	−1.14	0.06	1	Ref. 30
Kefir	−1.11	0.20	4	Ref. 30
Yogurt	−1.22	0.04	1	Ref. 30
Commercial milk	−1.00	0.01	4	Ref. 30
Ultrahigh-temperature milk	−1.19	0.28	5	Ref. 31
Cheese (gouda)	−1.11	0.02	3	Ref. 31
Cheese (emmentaler)	−1.05	0.26	1	Ref. 31
Cheese (brie)	−1.21	0.02	2	Ref. 31
BCR-380R (whole milk powder)	−1.10	0.10	16	This study
Average of cow dairy products	−1.13	0.13		(2 SD, *n* = 11)
Infant formulas				
Blédilait, 0–6 mo	−0.71	0.01	2	This study
Gallia, 0–6 mo	−0.62	0.22	3	This study
Gallia, premature/low-weight infant	−0.82	0.19	3	This study
Guigoz, 0–6 mo, antiregurgitation	−0.22	0.09	6	This study
Guigoz, 0–6 mo	−0.51	0.05	3	This study
Guigoz, premature/low-weight infant	−0.01	0.05	2	This study
Milumel, 6–12 mo	−0.62	0.10	3	This study
Modilac, 0–6 mo, antiregurgitation	−0.62	0.17	4	This study
Modilac, premature/low-weight infant	−0.81	0.13	4	This study
Nidal, 0–6 mo	−0.48	0.20	2	This study
Novalac, 0–6 mo, antiregurgitation	−0.25	0.13	3	This study
Nutricia, 0–12 mo, medical nutrition	−0.69	0.11	2	This study
Picot, 0–6 mo, medical nutrition	−0.58	—	1	This study
Picot, 6–12 mo, medical nutrition	−0.20	0.17	4	This study
Picot, 0–12 mo, lactose-free	−0.19	0.10	2	This study
Average of infant formulas	−0.49	0.51		(2 SD, *n* = 15)
Human breast milk				
Individual A (2 mo after birth), United Kingdom	−1.71	0.28	5	Ref. 30
Individual A (4 mo after birth) United Kingdom	−1.97	0.02	3	Ref. 30
Individual B (1 mo after birth), United Kingdom	−1.54	0.26	1	Ref. 30
Individual C (4 mo after birth), United Kingdom	−1.50	0.02	2	Ref. 30
French individual (1 wk after birth)	−1.63	0.13	5	This study
Average of breast milk	−1.67	0.37		(2 SD, *n* = 5)
Human whole blood				
Baseline patient 1, United States	−1.14	0.15	—	Ref. 47
Baseline patient 2, United States	−0.99	0.16	—	Ref. 47
Baseline patient 3, United States	−1.02	0.19	—	Ref. 47
Baseline patient 4, United States	−1.22	0.16	—	Ref. 47
Baseline patient 5, United States	−1.23	0.18	—	Ref. 47
Baseline patient 6, United States	−0.99	0.15	—	Ref. 47
Baseline patient 7, United States	−1.00	0.06	—	Ref. 47
Baseline patient 8, United States	−0.97	0.24	—	Ref. 47
Baseline patient 9, United States	−1.37	0.09	—	Ref. 47
Baseline patient 10, United States	−1.29	0.08	—	Ref. 47
Baseline patient 11, United States	−1.19	0.10	—	Ref. 47
Baseline patient 12, United States	−1.26	0.01	—	Ref. 47
Average of ref. 47 (United States)	−1.14	0.28		(2 SD, *n* = 12)
25-y-old male, France	−1.41	0.08	5	This study
39-y-old female, France	−1.43	0.12	9	This study
Average of this study (France)	−1.42	0.03		(2 SD, n = 2)
Average whole blood	−1.28	0.39		

Table S1. Cont.

Material	$\delta^{44/42}$Ca (relative to ICP Ca Lyon), ‰ ± 2 SD	*n*	Source
Average Western diet components			
Dairy products	−1.12	—	Ref. 32
Vegetables	−0.86	—	Ref. 32
Fruit	−0.86	—	Ref. 32
Cereal products	−0.80	—	Ref. 32
Meat	−0.56	—	Ref. 32
Fats	−1.02	—	Ref. 32
Water	−0.18	—	Ref. 32
Typical Western diet	−1.02	—	Ref. 32
Typical vegan diet	−0.83	—	Ref. 32

Table S2. Summary of statistical analyses performed on dataset between main groups

All data - $\delta^{44/42}Ca$

Groups: *prenatal - birth - postnatal - 7 to 15 yrs*

Welch's ANOVA: ***P* value =** **<0.0001** *** F =15.6**

Kruskal-Wallis: ***P* value =** **<0.0001** *** $\chi2$ = 39.8**

Paired Welch's t-test

Bonferroni p-value adjustment method

***P* values**	birth	postnatal	7 to 15 yrs
prenatal	1	**<0.0001**	**0.0017**
birth	-	**0.018**	**0.001**
postnatal	-	-	**0.17**

Paired Wilcoxon-Mann-Whitney test

Bonferroni p-value adjustment method

***P* values**	birth	postnatal	7 to 15 yrs
prenatal	1	**<0.0001**	**0.0001**
birth	-	**0.031**	**0.0021**
postnatal	-	-	**0.50**

Short breastfeeding (≤4 months) - $\delta^{44/42}Ca$

Groups: *prenatal - birth - postnatal - 7 to 15 yrs*

Welch's ANOVA: ***P* value =** **<0.0001** *** F =18.3**

Kruskal-Wallis: ***P* value =** **<0.0001** *** $\chi2$ = 13.9**

Paired Welch's t-test

Bonferroni p-value adjustment method

***P* values**	birth	postnatal	7 to 15 yrs
prenatal	**1**	**<0.0001**	**0.0002**
birth	-	**0.035**	**0.0094**
postnatal	-	-	**1**

Paired Wilcoxon-Mann-Whitney test

Bonferroni p-value adjustment method

***P* values**	birth	postnatal	7 to 15 yrs
prenatal	**1**	**<0.0001**	**<0.0001**
birth	-	**0.034**	**0.015**
postnatal	-	-	**1**

Long breastfeeding (>12 months) - $\delta^{44/42}Ca$

Groups: *prenatal - birth - postnatal - 7 to 15 yrs*

Welch's ANOVA: ***P* value =** **0.0002** *** F =15.9**

Kruskal-Wallis: ***P* value =** **0.0002** *** $\chi2$ = 20**

Paired Welch's t-test

Bonferroni p-value adjustment method

***P* values**	birth	postnatal	7 to 15 yrs
prenatal	**1**	**1**	**<0.0001**
birth	-	**1**	**0.0096**
postnatal	-	-	**<0.0001**

Paired Wilcoxon-Mann-Whitney test

Bonferroni p-value adjustment method

***P* values**	birth	postnatal	7 to 15 yrs
prenatal	**1**	**1**	**0.00013**
birth	-	**1**	**0.017**
postnatal	-	-	**<0.0001**

Short breastfeeding (≤4 months) - $\Delta^{44/42}Ca$

Groups: *prenatal - birth - postnatal*

Welch's ANOVA: ***P* value =** **<0.0001** *** F = 70.4**

Kruskal-Wallis: ***P* value =** **<0.0001** *** $\chi2$ = 67.9**

Paired Welch's t-test

Bonferroni p-value adjustment method

***P* values**	birth	postnatal
prenatal	**0.00086**	**<0.0001**
birth	-	**<0.0001**

Paired Wilcoxon-Mann-Whitney test

Bonferroni p-value adjustment method

***P* values**	birth	postnatal
prenatal	**0.00041**	**<0.0001**
birth	-	**0.0034**

Long breastfeeding (>12 months) - $\Delta^{44/42}Ca$

Groups: *prenatal - birth - postnatal*

Welch's ANOVA: ***P* value =** **0.76** ***NS,* F = 0.28**

Kruskal-Wallis: ***P* value =** **0.66** ***NS,* $\chi2$ = 0.84**

Paired Welch's t-test

Bonferroni p-value adjustment method

P values	*birth*	*postnatal*
prenatal	*1*	*1*
birth	-	*1*

Paired Wilcoxon-Mann-Whitney test

Bonferroni p-value adjustment method

P values	*birth*	*postnatal*
prenatal	*1*	*1*
birth	-	*1*

Table S3. Compilation of measured $\Delta^{44/42}Ca_{blood\text{-}diet}$ shifts ($\delta^{44/42}Ca_{blood} - \delta^{44/42}Ca_{diet}$) in mammals (32, 42, 44, 46, 47)

Mammal	$\Delta^{44/42}Ca_{blood\text{-}diet}$, ‰	*n*	Source
Horse	−0.30	1	Ref. 42
Seal	−0.16	1	Ref. 42
Minipig	−0.20	2	Ref. 32
Pig (sow)	−0.52	1	Ref. 46
Sheep	−0.34	4	Ref. 44
Human*	−0.26	14	Ref. 47 (baselines only) and this study
Average	−0.30 ± 0.13 (SD)		

*Estimated in humans using −1.02‰ estimated diet and −1.28‰ blood average composition.

Table S4. $\delta^{44/42}Ca$ values of standards as measured in this study (in per mil relative to ICP Ca Lyon standard) compared with previously published values (34, 37, 44, 46, 47)

Standard	Source	*n*	$\delta^{44/42}Ca$, ‰, ±2 SD relative to ICP Ca Lyon	
SRM1486 (cow bone meal)	This study, July 2015	17	−1.04	0.13
	This study, November 2015	27	−1.03	0.12
	This study, December 2015	22	−1.03	0.10
	This study, August 2016	29	−1.05	0.12
	This study, February 2017	31	−1.00	0.09
	This study, March 2017	21	−1.02	0.11
	This study, average of all sessions	147	−1.03	0.12
	Ref. 44	17	−0.96	0.14
	Ref. 34	120	−1.03	0.13
	Ref. 37	25	−1.04	0.11
SRM915b (Ca carbonate)	This study	4	−0.16	0.04
	Ref. 44	11	−0.12	0.07
	Ref. 34	4	−0.14	0.06
	Ref. 37	13	−0.15	0.11
SRM915a (Ca carbonate)	This study	5	−0.52	0.10
	Estimation from literature (37)	—	−0.52	0.08
SRM1400 (cow bone ash)				
Powder	Ref. 34, SRM1400	26	−1.24	0.13
Microsampled on sinter	This study, SRM1400 SPS 1	3	−1.23	0.08
	This study, SRM1400 SPS 2	5	−1.27	0.06
	Ref. 34, SRM1400 SPS	11	−1.18	0.16
BCR-380R (cow whole milk powder)	This study	16	−1.10	0.10
ICP1 Ca solution (46, 47)	This study	10	−0.20	0.10

Fig. S1. Three isotopes plot: $\delta^{43/42}Ca$ (per mil) as a function of $\delta^{44/42}Ca$ (per mil) relative to ICP Ca Lyon. Ca isotope composition falls on a line with a *y* axis intercept of 0.000 ± 0.016 (2 SE), indistinguishable from theoretical 0‰ intercept, and a slope of 0.507 ± 0.010 (2 SE) indistinguishable from 0.507 predicted slope according to exponential law linear approximation of mass-dependent fractionation. Error bars correspond to average 2 SD precision on $\delta^{44/42}Ca$ (per mil) and $\delta^{43/42}Ca$ (per mil). Black triangles are samples measured in this study; red triangles are standards. The blue lines delimit the prediction interval, and the red lines correspond to the 95% confidence interval on the regression line.

Fig. S1

Fig. S2. Distribution of $\delta^{44/42}$Ca values (per mil, ICP Ca Lyon) in human deciduous and wisdom tooth enamel in the context of earth-surface natural variability (30, 33, 70). Human deciduous enamel spreads at the very lower end of natural variability, among the most ^{44}Ca-depleted compositions ever measured. The "Animals" category encompasses all accounted-for $\delta^{44/42}$Ca values of animal and human tissues and excretion, including urine, among the most ^{44}Ca-enriched published values.

Fig. S2

Fig. S3. $\delta^{44/42}$Ca values (per mil, ICP Ca Lyon) of prenatal, birth, and postnatal enamel for each individual, sorted according to age at cessation of breast-feeding. Each individual is associated with *P* values for Kruskal–Wallis test for all categories (Kr-W.) and Wilcoxon–Mann–Whitney for comparison of prenatal and postnatal enamel values (Wilcox.). NS, nonsignificant *P* value; $*P = 0.01–0.05$; $**P = 0.001–0.01$; and $***P < 0.001$.

Fig. S3

Fig. S4. Annotated pictures of teeth and sampling spots. Red areas correspond to sampling spots. Green lines represent neonatal lines, yellow solid lines represent accentuated markings, yellow dashed lines represent inferred isochronous lines, and black lines represent main prism orientation along which distances to neonatal lines were measured.

Fig. S4

Dataset S1. All measured $\delta^{44/42}$Ca values together with global information on each individual, tooth, and sample

Dataset S1

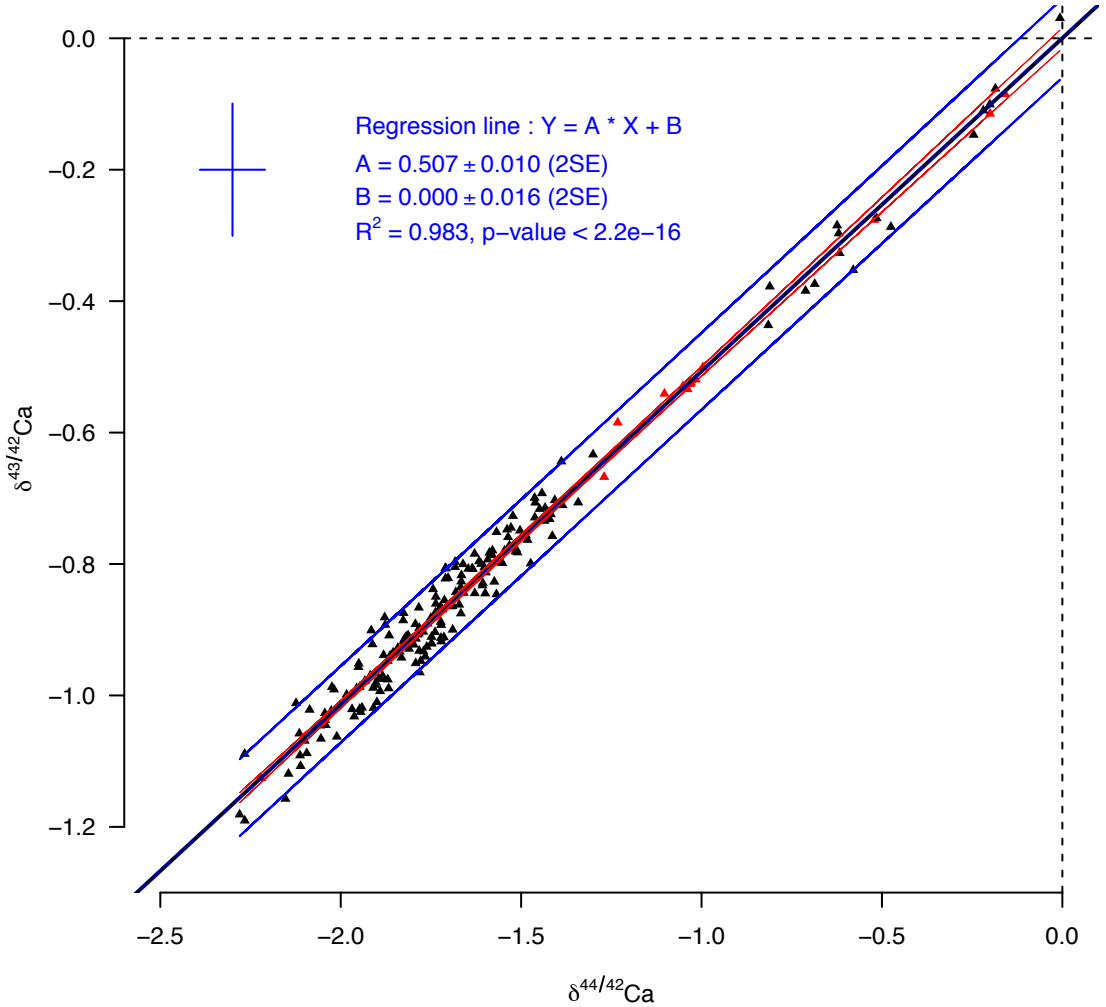
Regression line : Y = A * X + B
A = 0.507 ± 0.010 (2SE)
B = 0.000 ± 0.016 (2SE)
R2 = 0.983, p−value < 2.2e−16
δ43/42Ca
δ44/42Ca
0.0
−0.2
−0.4
−0.6
−0.8
−1.0
−1.2
−2.5
−2.0
−1.5
−1.0
−0.5
0.0

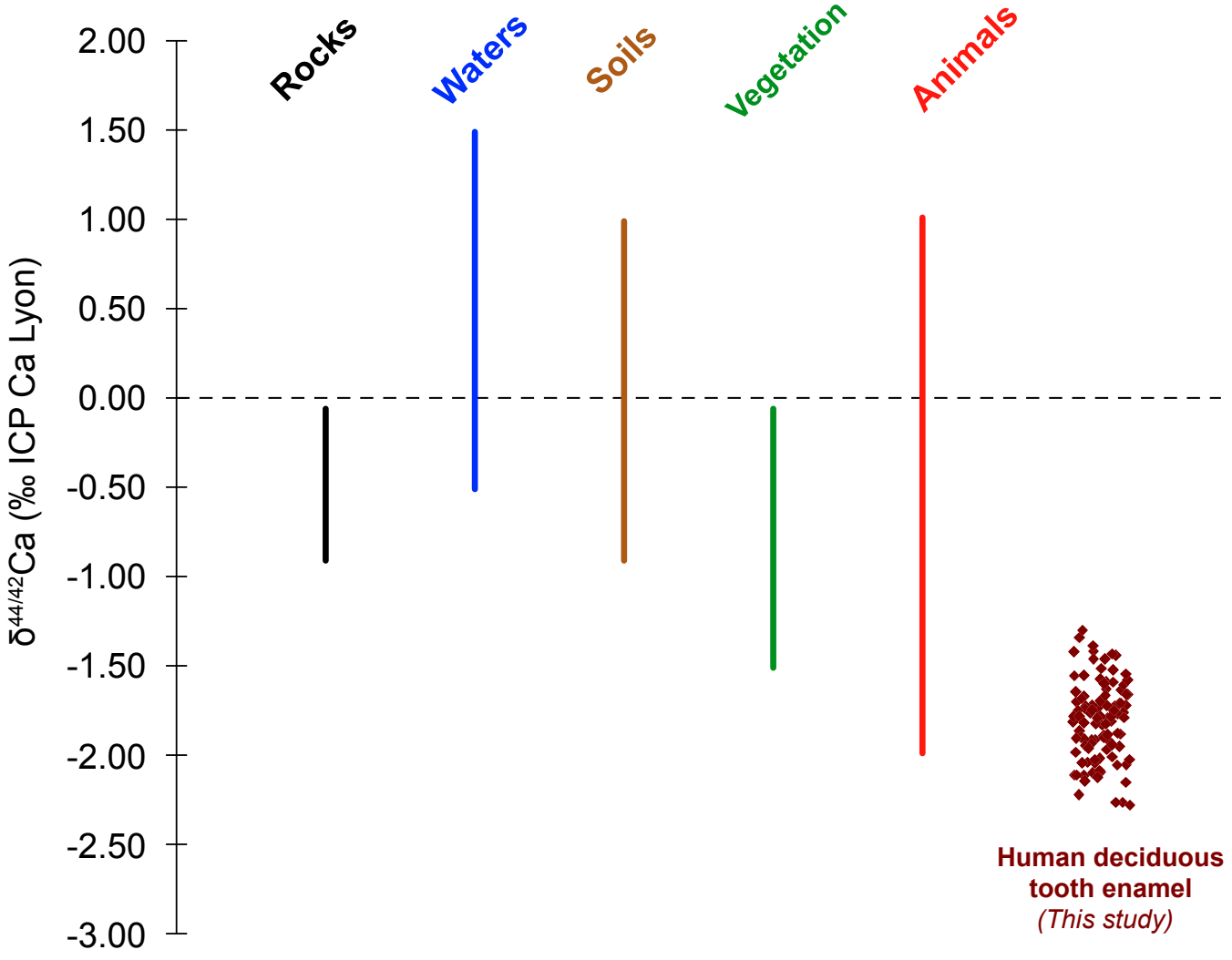
Rocks
Waters
Soils
Vegetation
Animals
2.00
1.50
1.00
0.50
0.00
-0.50
-1.00
-1.50
-2.00
-2.50
-3.00
δ44/42Ca (‰ ICP Ca Lyon)
Human deciduous tooth enamel
(This study)

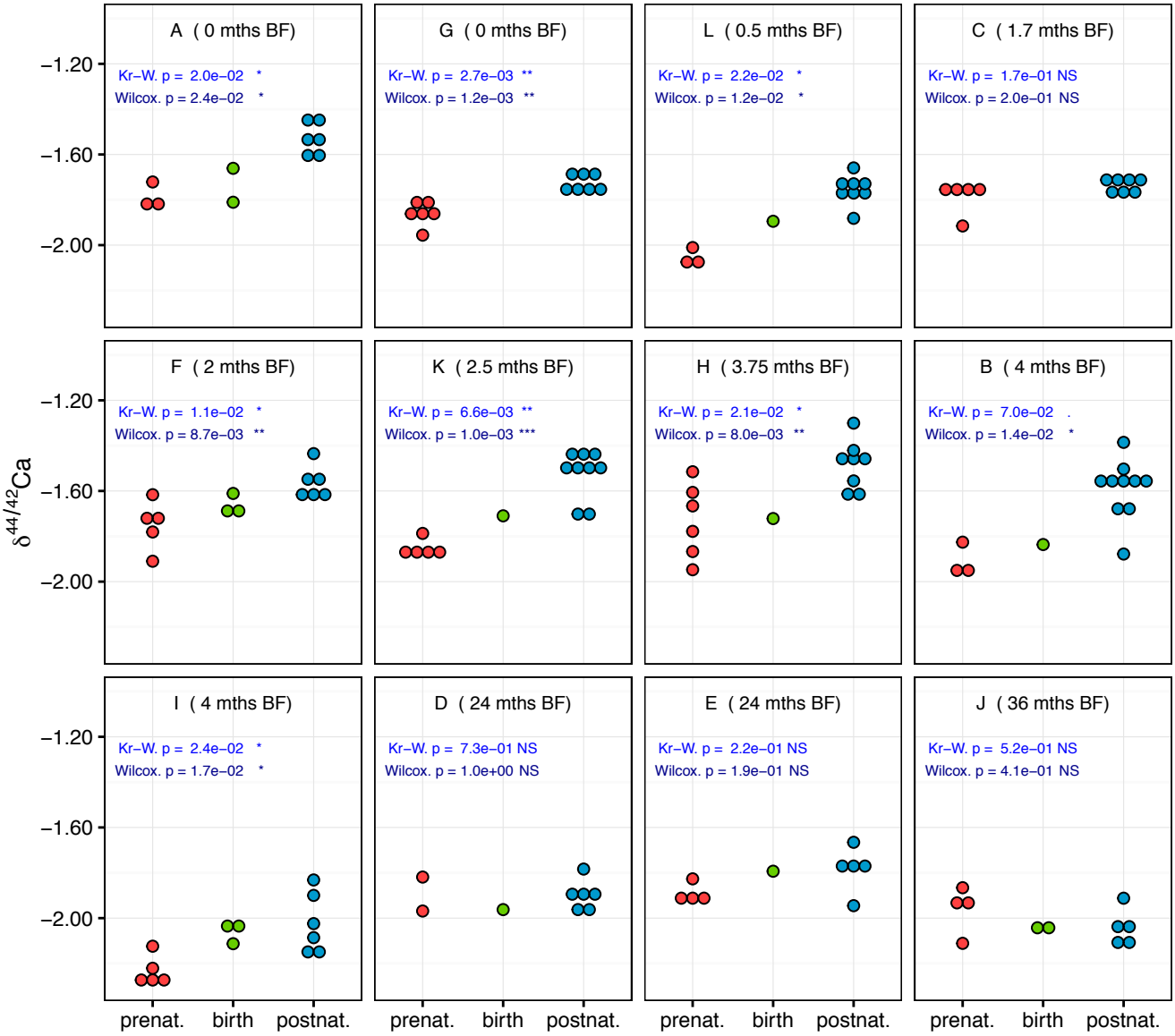
A (0 mths BF)
Kr–W. p = 2.0e–02 *
Wilcox. p = 2.4e–02 *
G (0 mths BF)
Kr–W. p = 2.7e–03 **
Wilcox. p = 1.2e–03 **
L (0.5 mths BF)
Kr–W. p = 2.2e–02 *
Wilcox. p = 1.2e–02 *
C (1.7 mths BF)
Kr–W. p = 1.7e–01 NS
Wilcox. p = 2.0e–01 NS
F (2 mths BF)
Kr–W. p = 1.1e–02 *
Wilcox. p = 8.7e–03 **
K (2.5 mths BF)
Kr–W. p = 6.6e–03 **
Wilcox. p = 1.0e–03 ***
H (3.75 mths BF)
Kr–W. p = 2.1e–02 *
Wilcox. p = 8.0e–03 **
B (4 mths BF)
Kr–W. p = 7.0e–02 .
Wilcox. p = 1.4e–02 *
I (4 mths BF)
Kr–W. p = 2.4e–02 *
Wilcox. p = 1.7e–02 *
D (24 mths BF)
Kr–W. p = 7.3e–01 NS
Wilcox. p = 1.0e+00 NS
E (24 mths BF)
Kr–W. p = 2.2e–01 NS
Wilcox. p = 1.9e–01 NS
J (36 mths BF)
Kr–W. p = 5.2e–01 NS
Wilcox. p = 4.1e–01 NS
δ44/42Ca
−1.20
−1.60
−2.00
prenat.
birth
postnat.

2mm

A - c’

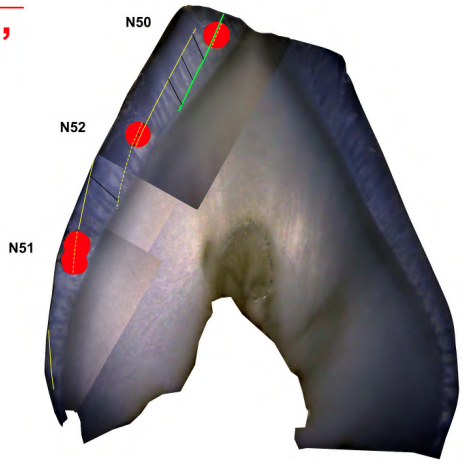

2mm

A - i^{1}

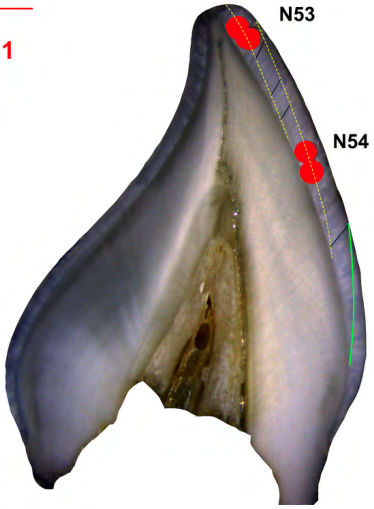

2mm

A - m^{1}

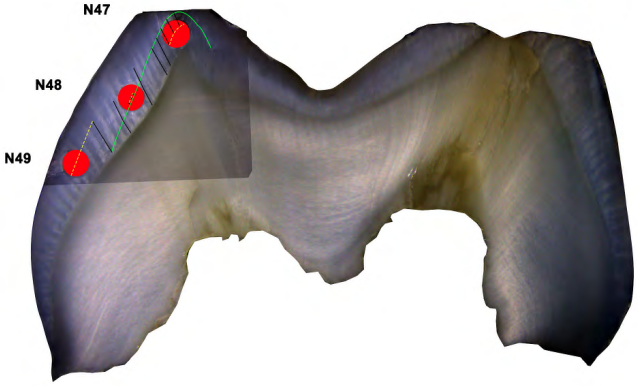

2mm

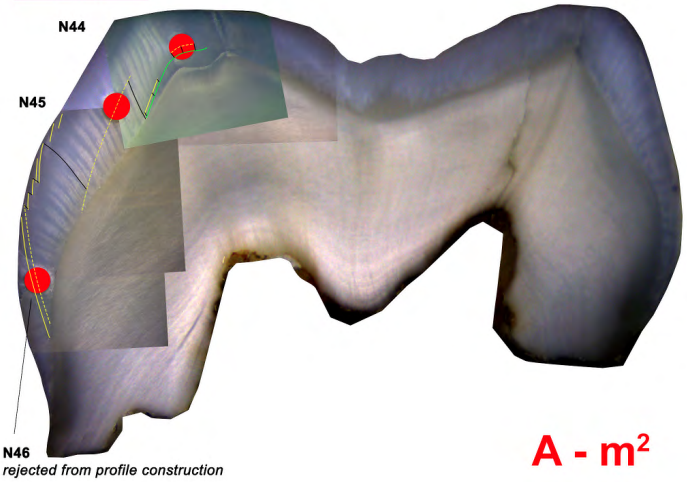

A - m^{2}

2mm

B - c’

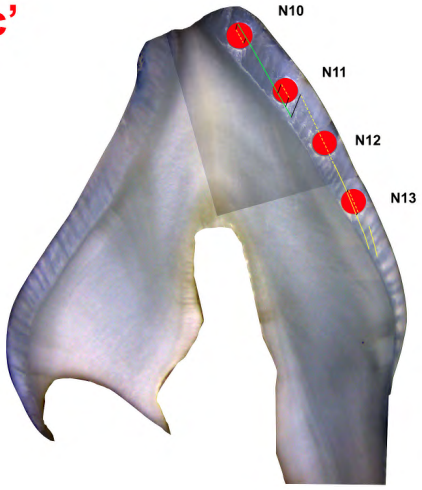

2mm

B - i¹

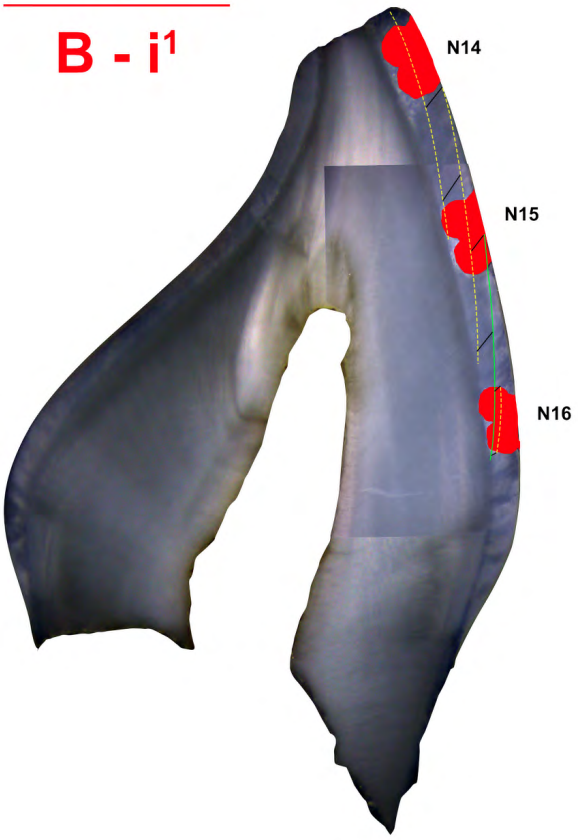

2mm

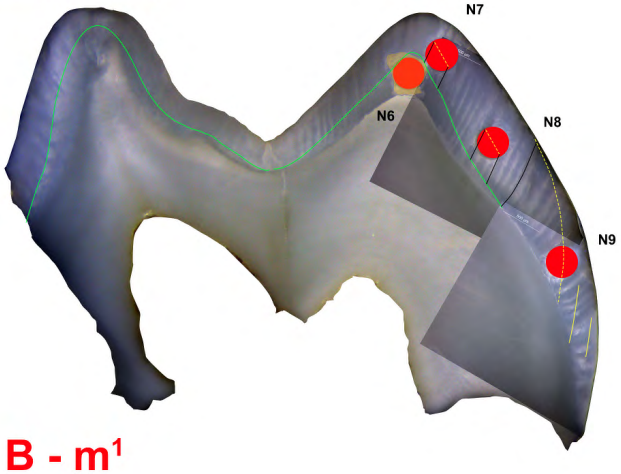

B - m¹

2mm

B - m²

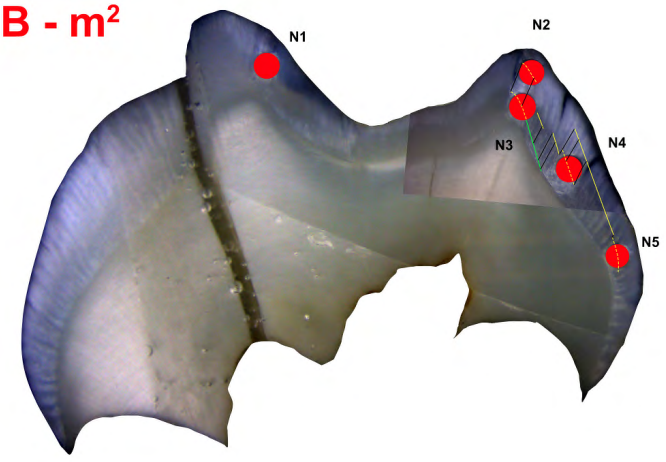

2mm

C - c’

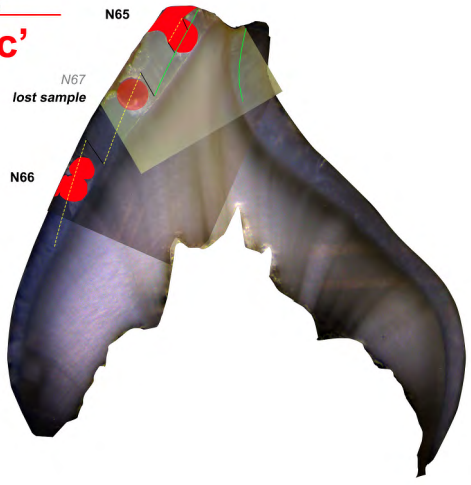

2mm

C - i^1

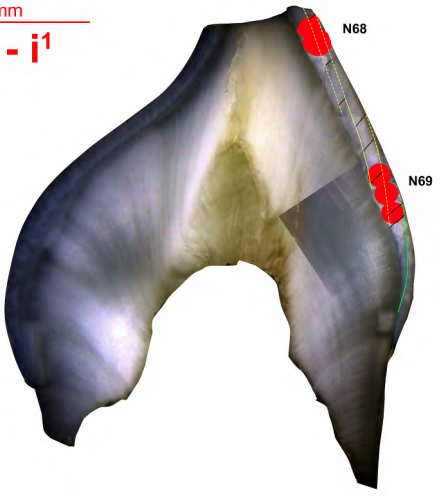

1mm

C - m$_1$

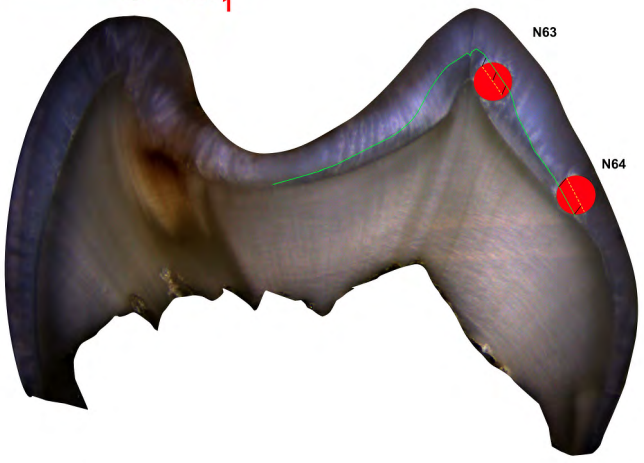

2mm

C - m^1

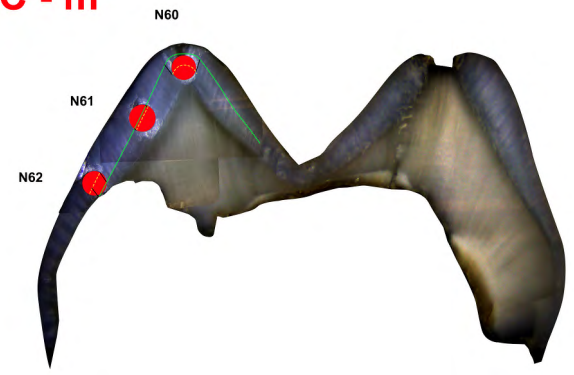

2mm

C - m^2

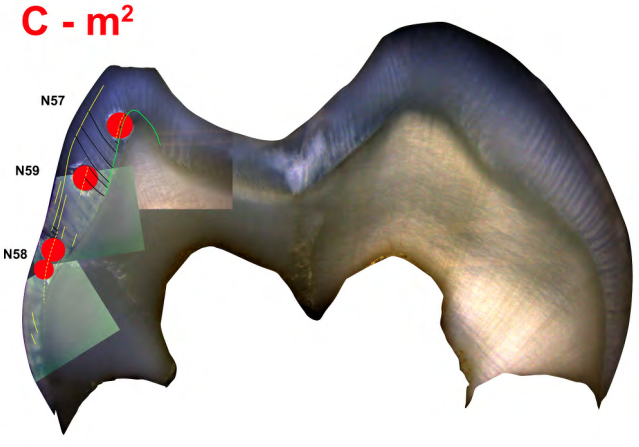

250µm

D - m_1 (L)

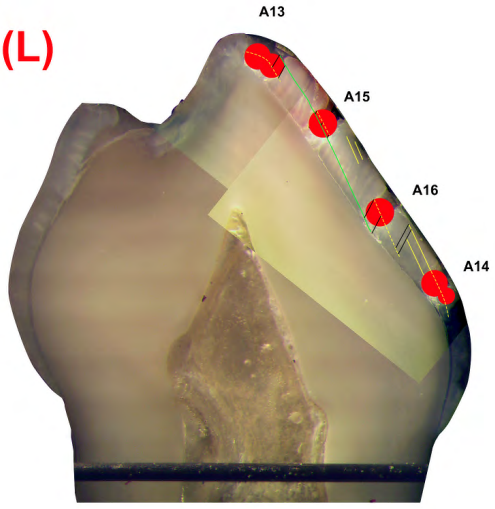

250µm

D - m_1 (R)

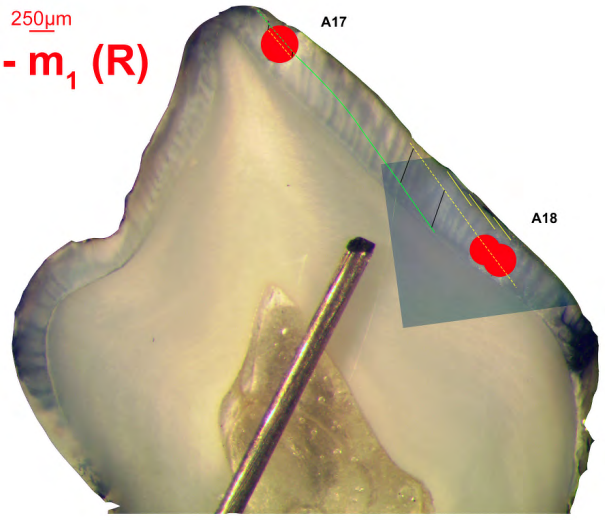

250µm

D - m^1 (L)

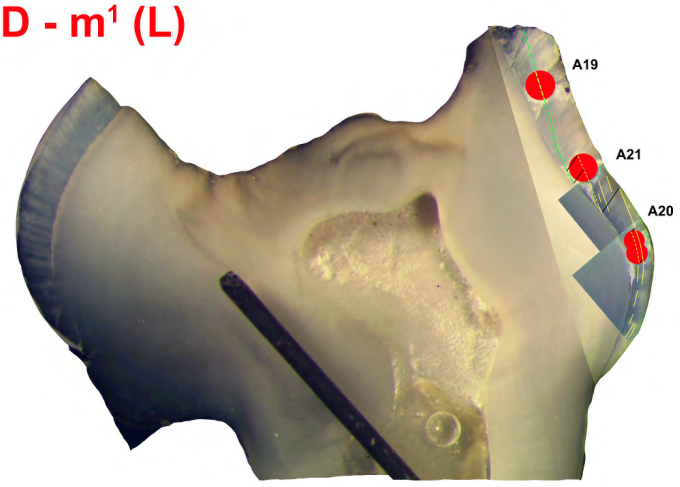

250µm

E - i

250µm

E - m_1

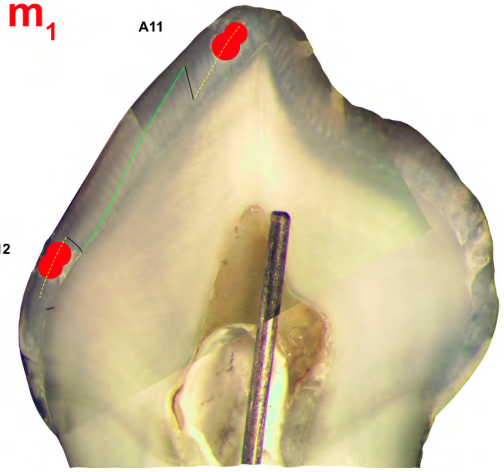

250µm

E - m_2

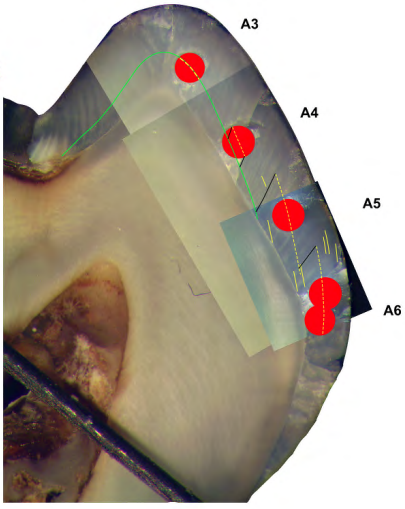

250µm E - m^1

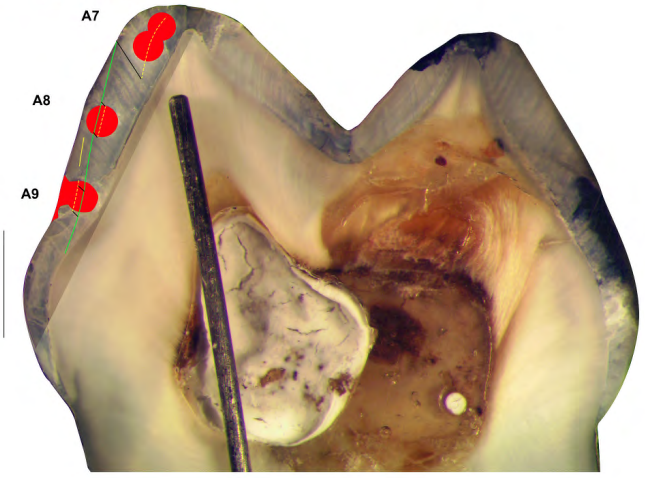

2mm

F - c’

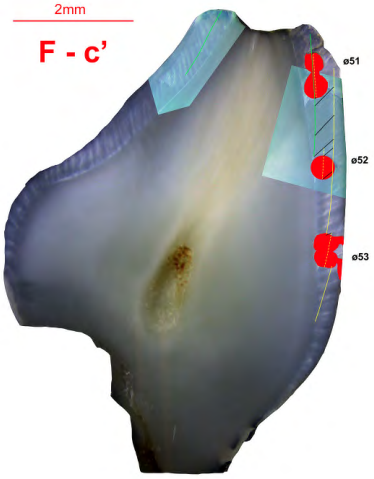

2mm

F - i¹

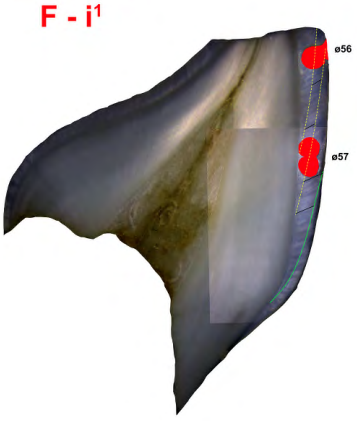

2mm

F - i²

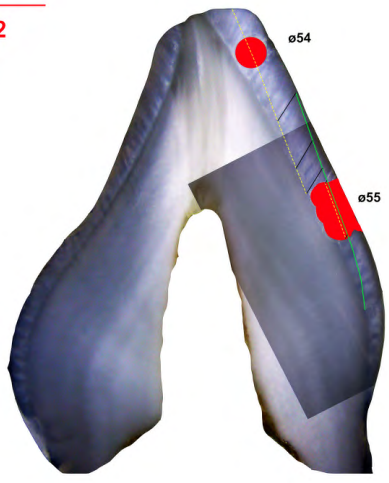

JGd
di^2 R

2mm

F - m¹

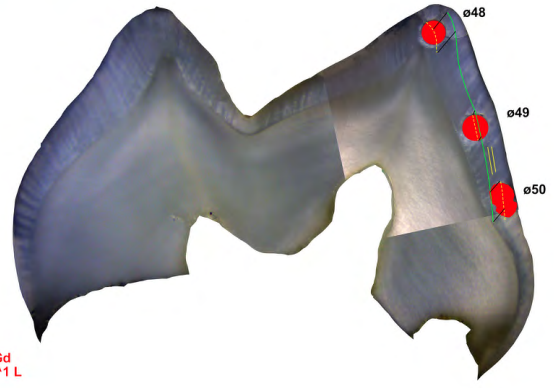

JGd
dm^1 L

2mm

F - m²

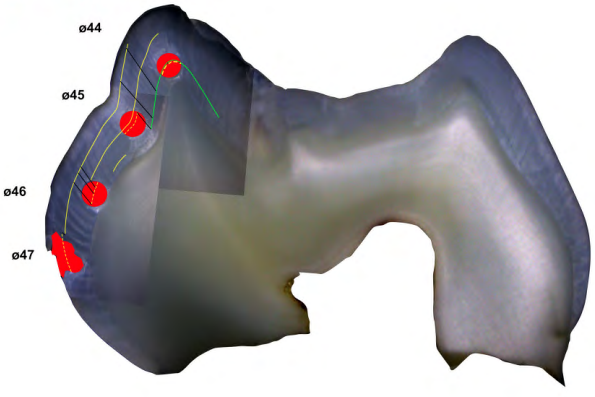

2mm

G - c’

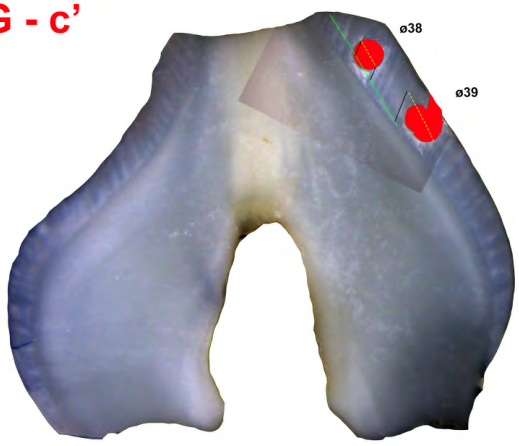

2mm

G - i^{1}

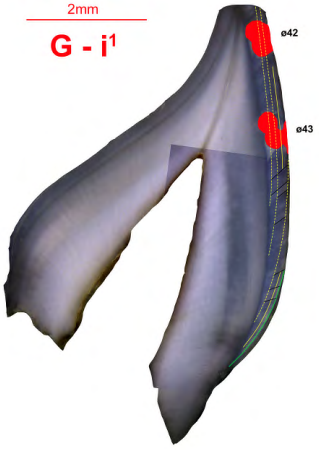

1mm

G - i^{2}

2mm

G - m^{1}

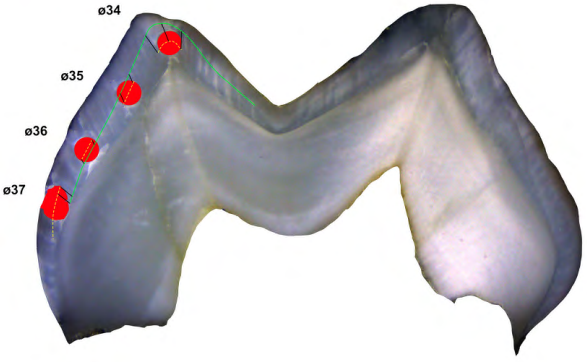

2mm

G - m^{2}

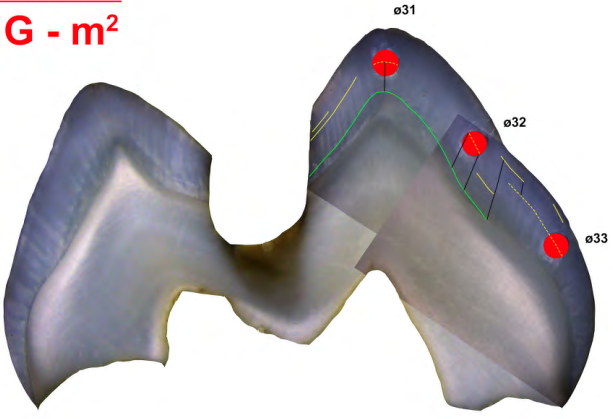

1mm

H - c’

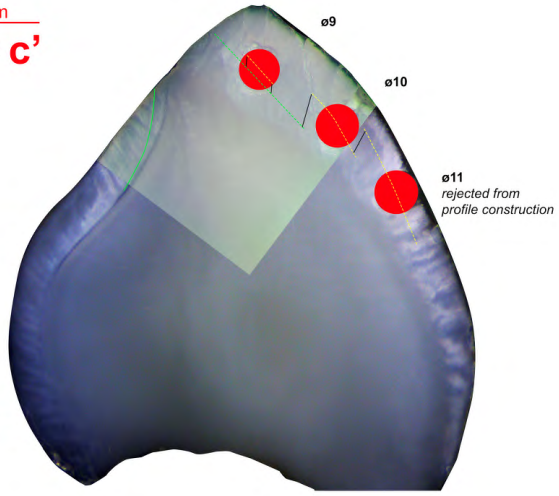

1mm

H - i¹

2mm

H - i²

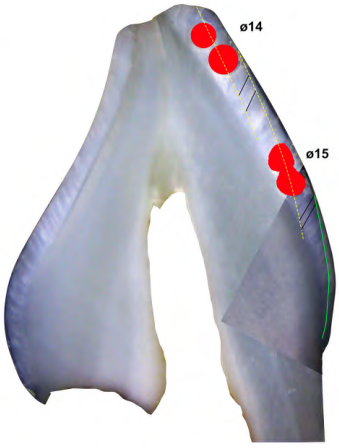

2mm

H - m¹

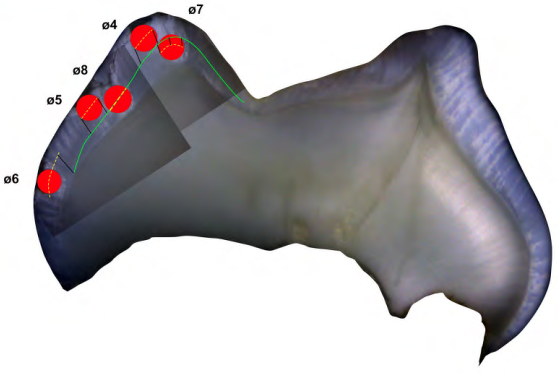

250µm

H - m²

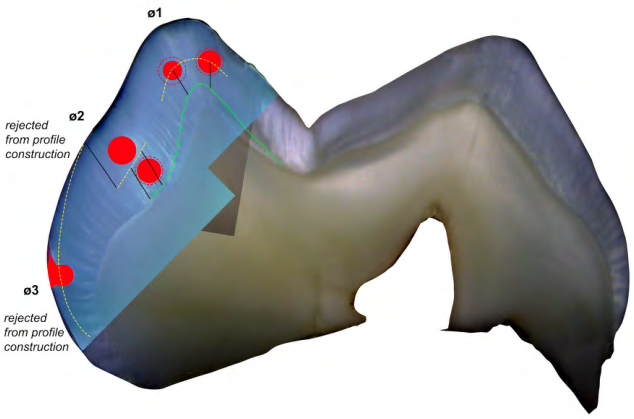

2mm

I - c’

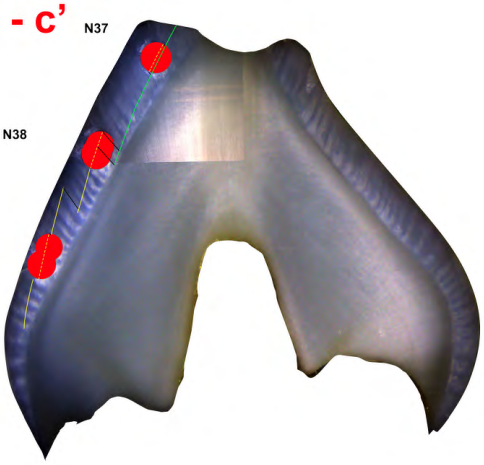

1mm

I - i¹

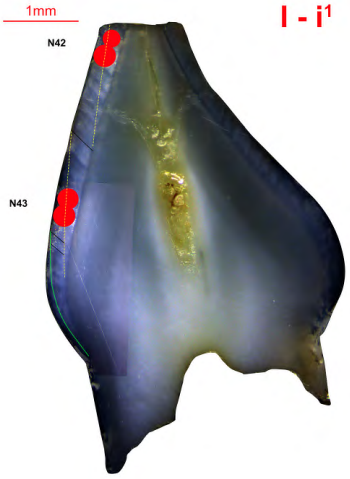

1mm

I - i²

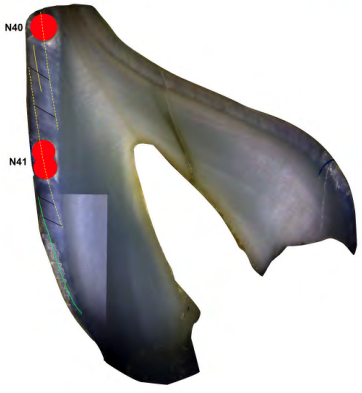

2mm

I - m_1

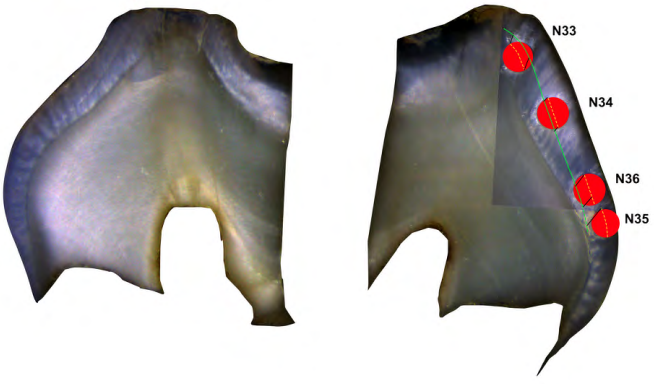

2mm

I - m¹

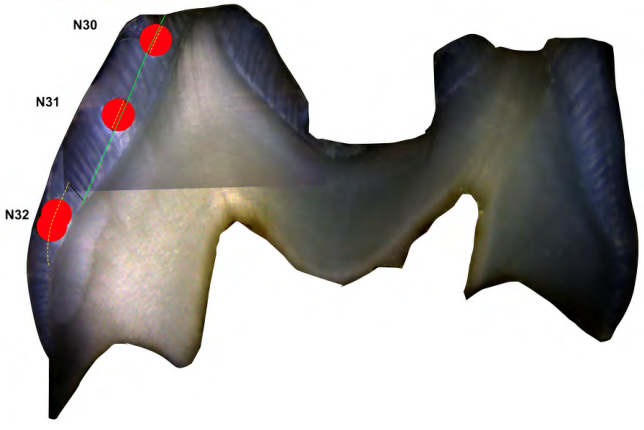

2mm

J - c,

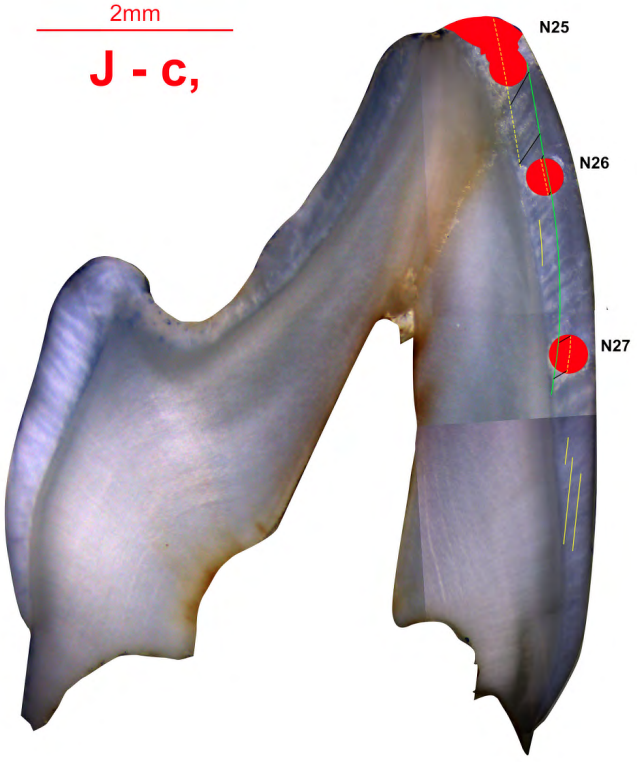

J - m_1

2mm

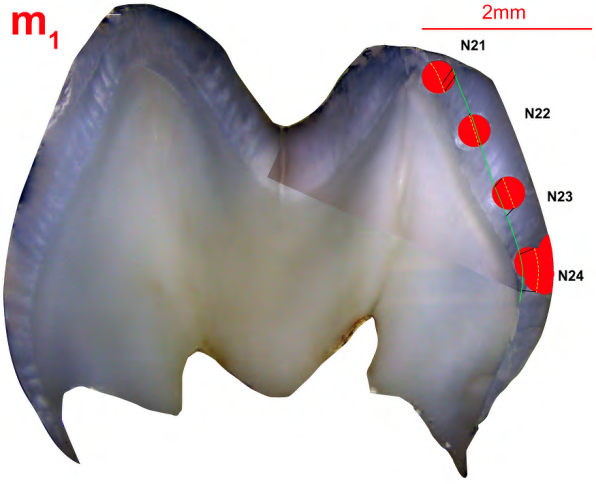

2mm

J - m^1

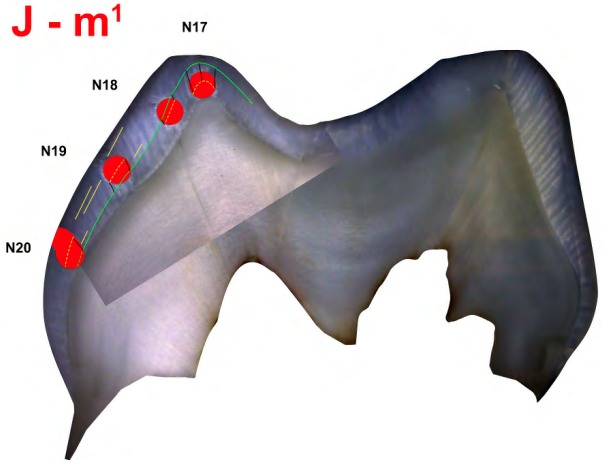

2mm

K - c’

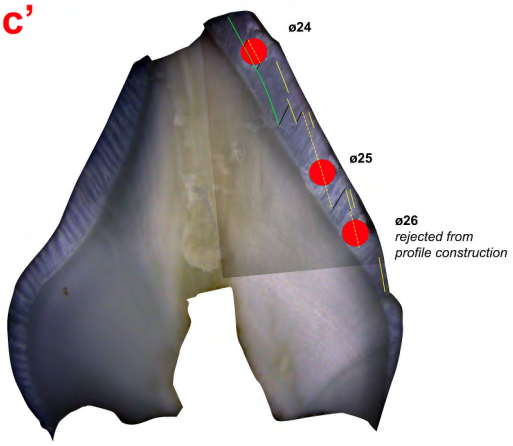

2mm

K - i^1

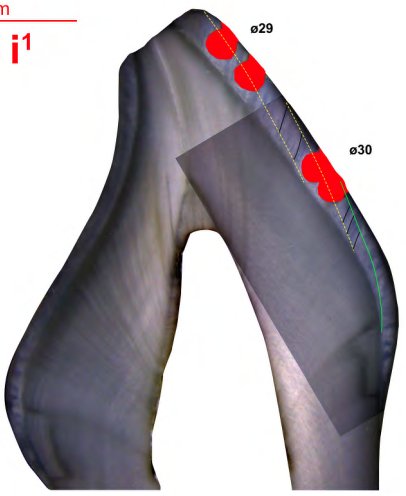

2mm

K - i^2

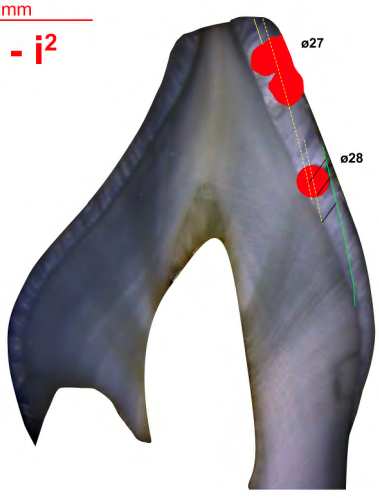

2mm

K - m^1

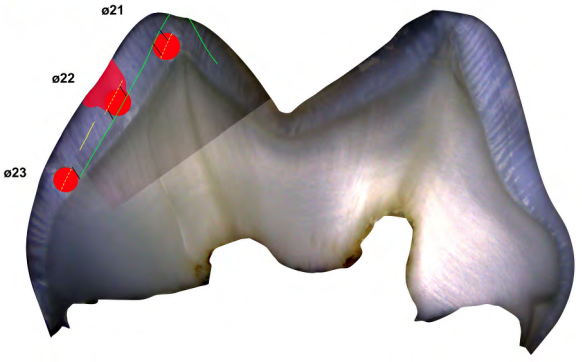

2mm

K - m^2

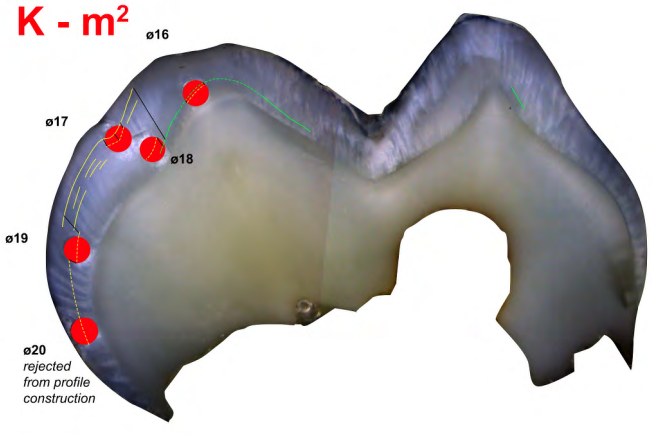

2mm

L - i^1

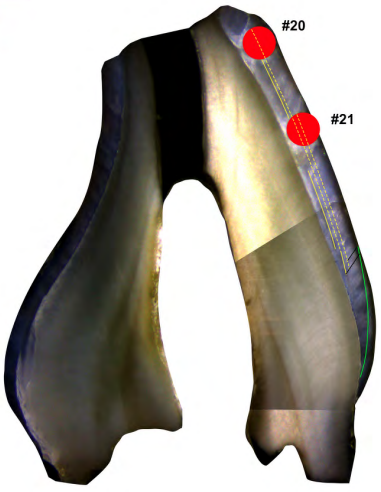

2mm

L - m^1

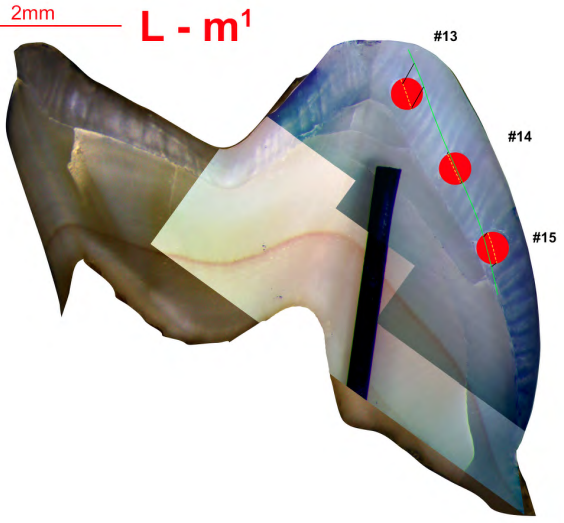

2mm

L - m^2